SCIENCE CHINA PRESS

SCIENCE CHINA Chemistry
https://doi.org/10.1007/s11426-026-3480-3

REVIEWS

Catalytic enantioselective synthesis via axial chirality transfer of transient atropisomers

Pei-Chao Zhang[1*], Wen-Wen Zhang[1], Bing Xu[1], Yan Zou[1], Qingjie Zhao[1*] & Junliang Zhang[2*]

[1]The Center for Basic Research and Innovation of Medicine and Pharmacy (MOE), School of Pharmacy, Naval Medical University (Second Military Medical University), Shanghai 200433, China
[2]Department of Chemistry, Fudan University, Shanghai 200438, China
*Corresponding authors (email: pczhang@smmu.edu.cn; qjzhao@smmu.edu.cn; junliangzhang@fudan.edu.cn)

Received 14 March 2026; Accepted 14 April 2026; Published online 21 August 2026

Abstract Atropisomers have attracted growing interest in synthetic and medicinal chemistry. Nevertheless, transient atropisomeric intermediates are often overlooked in catalytic asymmetric synthesis, and the chirality transfer processes mediated by these species have thus not been systematically explored or thoroughly studied. The catalytic enantioselective synthesis via a transient axial chirality transfer strategy effectively overcomes the reliance of traditional methods on pre-synthesized chiral substrates. By virtue of the precise stereinduction by chiral catalysts to generate transient axial chirality relays, it enables the efficient conversion of racemic or prochiral precursors into chiral functional molecules. This review focuses on metal-catalyzed enantioselective reaction pathways for the transfer of transient atropisomer axial chirality to central chirality and/or axial chirality. Through a systematic overview of the latest advances, current challenges, and future perspectives, this review is intended to offer comprehensive guidance and fresh perspectives for researchers in related fields, and to foster the development and application of novel chirality transfer strategies in asymmetric catalysis.

Keywords axial-to-central chirality transfer, axial-to-axial chirality transfer, transient atropisomeric intermediates, quaternary carbon stereocenters, catalytic asymmetric dearomatization

1 Introduction

Atropisomers represent a distinct subclass of axially chiral compounds, and are formally defined as conformational stereoisomers that persist under ambient conditions due to a sufficiently high rotational barrier about a σ single bond ($\Delta E_{rot} \geqslant 20$ kcal/mol) [1,2]. By general academic consensus, a conformer is only classified as an atropisomer when its racemization half-life ($t_{1/2}$) >1000 s [3]. Over the past two decades, atropisomerism has demonstrated exceptionally important research value and application prospects in synthetic chemistry, medicinal chemistry, and chiral materials science, with related research undergoing explosive growth [4]. Since the first report of atropisomers in 1922 [5], the vast majority of studies have focused on the asymmetric construction, property development, and application expansion of thermodynamically stable atropisomers. However, transient atropisomeric intermediates are readily overlooked in catalytic asymmetric synthesis, and the chirality transfer processes mediated by these species have consequently not been thoroughly investigated.

Chirality transfer [6–20], also referred to as "chirality conversion", "chirality exchange", "transfer of asymmetry", "self-immolative chirality transfer", or "traceless chirality transfer", is defined as a chemical process in which an original stereogenic element is erased while a new stereogenic element of a different nature is simultaneously constructed. Typical examples include chirality transfer from central-to-central [8], central-to-axial [9–13], central-to-helical [14], central-to-planar [15], axial-to-central [16–18], axial-to-axial [19], and axial-to-helical chirality [20]. Traditional chirality transfer strategies (Figure 1a) and chiral substrate-induced strategies (Figure 1b) represent the classic paradigm for chiral construction developed in the early stage of asymmetric synthesis. The core of such strategies relies on pre-synthesized enantiopure chiral substrates as the sole chiral source. Through the inherent stereochemical moieties of the substrates (*e.g.*, pre-existing central chirality or axial chirality), the chiral information is precisely transferred to the new chiral site in a stereospecific manner during subsequent chemical transformations, including functionalization and cyclization, thus enabling the construction of target chiral molecules. Nevertheless, these strategies are highly dependent on pre-synthesized enantiopure substrates, whose preparation usually requires tedious multi-step reactions or chiral resolution.

Such processes suffer from cumbersome synthetic steps, low atom economy, and limited substrate scope, making it difficult to adapt to the efficient synthesis of complex functional molecules.

In recent years, with the growing demand for efficient and atom-economical chiral construction methods in the field of asymmetric synthesis [21,22], catalytic enantioselective synthesis via chirality transfer has emerged as a highly attractive cutting-edge research focus in chiral synthesis. (Figure 1c). This strategy uses readily available and low-cost racemic or prochiral precursors as substrates. Through precise stereoinduction by a chiral catalyst, configurationally tunable transient atropisomeric intermediates are generated *in situ*, which transfer chiral information to the target chiral site with high fidelity. This strategy is particularly well-suited for the construction of chiral spirocycles that are difficult to access via traditional methods. It breaks the dependence of traditional chirality transfer on pre-synthesized enantiopure chiral substrates, and combines excellent step economy with high

Citation: Zhang PC, Zhang WW, Xu B, Zou Y, Zhao Q, Zhang J. Catalytic enantioselective synthesis via axial chirality transfer of transient atropisomers. *Sci China Chem*, https://doi.org/10.1007/s11426-026-3480-3

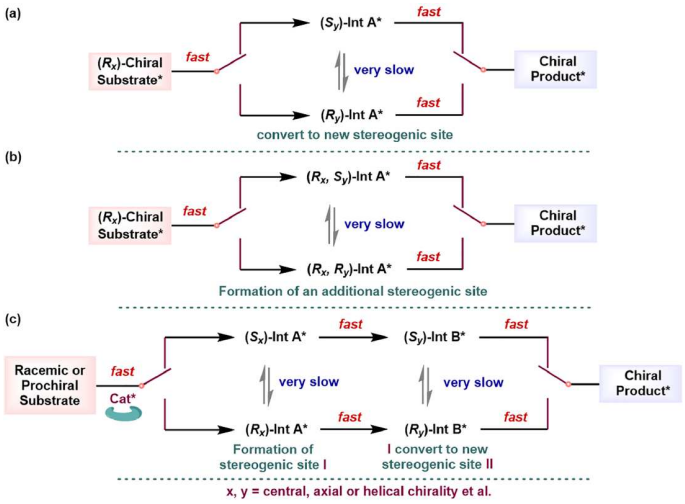

Figure 1 (Color online) The concept of asymmetric synthesis. (a) Traditional chirality transfer relies on pre-synthesized enantiopure chiral substrates. (b) Chiral substrate-induced asymmetric synthesis. (c) Catalytic enantioselective synthesis via transient chirality transfer with racemic/prochiral precursors.

stereoselectivity.

Catalytic enantioselective synthesis via transient atropisomer axial chirality transfer has emerged as a powerful tool for stereocontrol in asymmetric synthesis. This field was founded in 2015 by Luan *et al.* [23] and You *et al.* [24], back-to-back seminal *J. Am. Chem. Soc.* works, which first established the core concept and laid the foundational framework. Since then, diverse elegant transient axial chirality transfer strategies (*Luan-You chirality transfer*) have been developed via diverse reaction pathways, including deprotonation, reductive elimination, alkene insertion, carbonyl insertion, imine insertion, nucleophilic attack, oxidation, isomerization, and C–H insertion, enabling the efficient synthesis of a broad range of skeletons bearing quaternary/tertiary carbon stereocenters. Meanwhile, the scope of research on atropisomer axial chirality transfer has been extended to axial-to-axial chirality transfer via reductive elimination or electrophilic attack, thereby providing novel methodologies for the synthesis of low-stability axially chiral compounds. In this review, these reactions are categorized into two major classes based on the reaction types involved in the transient chirality transfer process, as illustrated in Figure 2.

Transient atropisomeric intermediates are defined as active species generated *in situ* during a reaction, which feature atropisomeric axial chirality. Unlike thermodynamically stable atropisomers, they retain configurational stability over the reaction timescale and act as the core relay for chiral induction and stereochemical information transfer. However, the configurational stability of transient atropisomeric intermediates is entirely dependent on the rotational energy barrier of the axial σ-bond. Such intermediates generally exhibit intrinsic features of short lifetime, low *in-situ* concentration, and easy racemization, rendering them difficult to be directly captured and accurately characterized by conventional mechanistic research techniques, including *in-situ* spectroscopy and single-crystal X-ray diffraction. Consequently, in reaction mechanism studies, the chirality transfer process mediated by these intermediates is often simplified to an ordinary transition state effect. Their core role in stereoselectivity control is highly prone to being underestimated, or even completely overlooked, and the corresponding systematic mechanistic elucidation remains far from comprehensive. Despite these remarkable achievements in this field, to the best of our knowledge, no comprehensive review has yet been published that systematically summarizes the research advances in this specific area. The catalytic enantioselective construction of atropisomers has long been a core and enduring challenge as well as a key research objective for organic chemists. Over the past two decades, numerous research highlights and review articles have been published in the relevant field [25–28], yet none have adequately emphasized transient atropisomeric intermediates or their role in mediating catalytic enantioselective

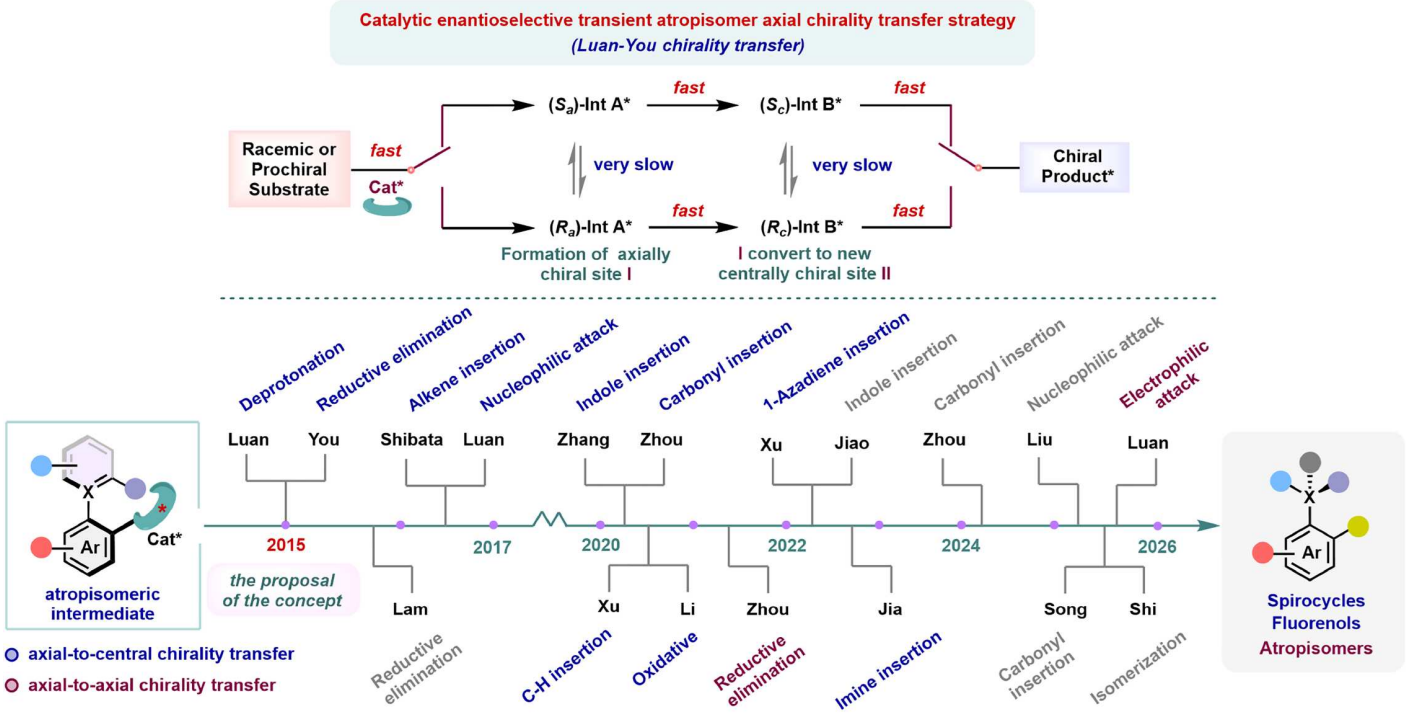

Figure 2 (Color online) The strategies used in this review for the catalytic enantioselective synthesis via transient atropisomer axial chirality transfer to synthesize chiral spirocycles, fluorenols and/or atropisomers.

synthesis via chirality transfer processes. On the other hand, several reviews have elaborated on chiral substrate-driven chirality transfer strategies from diverse research perspectives [9–14,16–18,20]. While comprehensive reviews from Nechab *et al.* [16], Franz and Neff [17], and Murai [18] have systematically delineated various chiral substrate-driven strategies for axial-to-central chirality transfer reactions, none of these prior works have addressed the catalytic enantioselective synthesis via the transient axial chirality transfer strategy that is the focus of this review. In light of the research landscape outlined above, we believe this comprehensive and timely review is warranted. It systematically summarizes the established asymmetric synthetic strategies based on catalytic enantioselective synthesis via transient axial chirality transfer, highlights the latest advances in this field, identifies promising yet underexplored opportunities for chirality transfer, and aims to inspire the development of more innovative and efficient chirality transfer strategies. To facilitate readers' understanding of the relevant content and advance the design and development of new reactions in the future, this review categorizes and elaborates on the reactions in accordance with the reaction types of the transient chirality transfer process involved in the design and development of the reported reactions.

2 Catalytic enantioselective synthesis via transient axial-to-central chirality transfer

2.1 Via deprotonation

Dynamic kinetic asymmetric transformation (DYKAT) is a powerful tool for converting racemic substrates to single enantiopure products [29–32], yet it has long been unsuccessfully applied to axial-to-central chirality transfer in biaryl systems. In 2015, Luan *et al.* [23] reported the first Pd-catalyzed DYKAT reaction of racemic biaryls, pioneering an economical synthetic pathway from racemic biaryls to chiral spirocycles (Figure 3) [33–35], and overcoming the long-standing bottleneck that axial-to-central chirality transfer strategies rely on pre-synthesized enantiopure atropisomeric substrates. To date, this seminal work remains a key reference for research on transient axial-to-central chirality transfer.

This study constructed a Pd/N-heterocyclic carbene (**NHC***) chiral catalytic system: using $Pd(OAc)_2$ as the optimal catalyst precursor, C_2-symmetric chiral **NHC** as the key ligand, NaO^{t}Bu as the base, and KI as an additive, the asymmetric spiroannulation of 4-(2-bromophenyl)naphthols **1** with internal alkynes **2** was achieved in tetrahydrofuran (THF) at 80 °C. This system effectively addresses the key limitations of traditional reactions—without the need for pre-synthesized chiral biaryls, it directly uses cheap racemates as raw materials, achieving yields of up to 98% and enantioselectivities of up to 94% enantiomeric excess (ee), demonstrating excellent catalytic performance. In terms of substrate scope, the reaction shows excellent compatibility with biaryl substrates bearing various substituents, including electron-donating groups (methyl, methoxy) and electron-withdrawing groups (trifluoromethyl, cyano, ester). Substrates with large steric hindrance (*ortho*-disubstituted), dihalogen-substituted substrates, and heterocyclic derivatives all undergo the reaction efficiently. Alkyne substrates cover symmetric aryl alkynes, heterocyclic alkynes, dialkyl alkynes, and alkynes with unsaturated functional groups, with regioselectivities ranging from 1.3:1 to 2:1 regiisomeric ratio (rr).

Lan and co-workers [36] confirmed via density functional theory (DFT) calculations that the optimal reaction pathway follows oxidative addition—alkyne insertion—deprotonation—reductive elimination. Pd(0) first undergoes oxidative addition with aryl bromide **1a** to form an aryl Pd(II) intermediate; the subsequent alkyne **2a** insertion into the Pd–C bond is both the rate-determining step and the enantioselectivity-determining step. The subsequent deprotonation and reductive elimination proceed rapidly to complete the catalytic cycle. The racemization barrier between intermediate Int-A and its enantiomer is lower than the insertion barrier, allowing rapid interconversion, while the racemization barrier of the intermediate after alkyne insertion is higher than that of the subsequent steps, ensuring the fidelity of chirality transfer. Noncovalent interaction analysis and transition state overlay analysis further confirm that the steric repulsion between the naphthol moiety and the chiral **NHC** ligand is the core origin of stereocontrol.

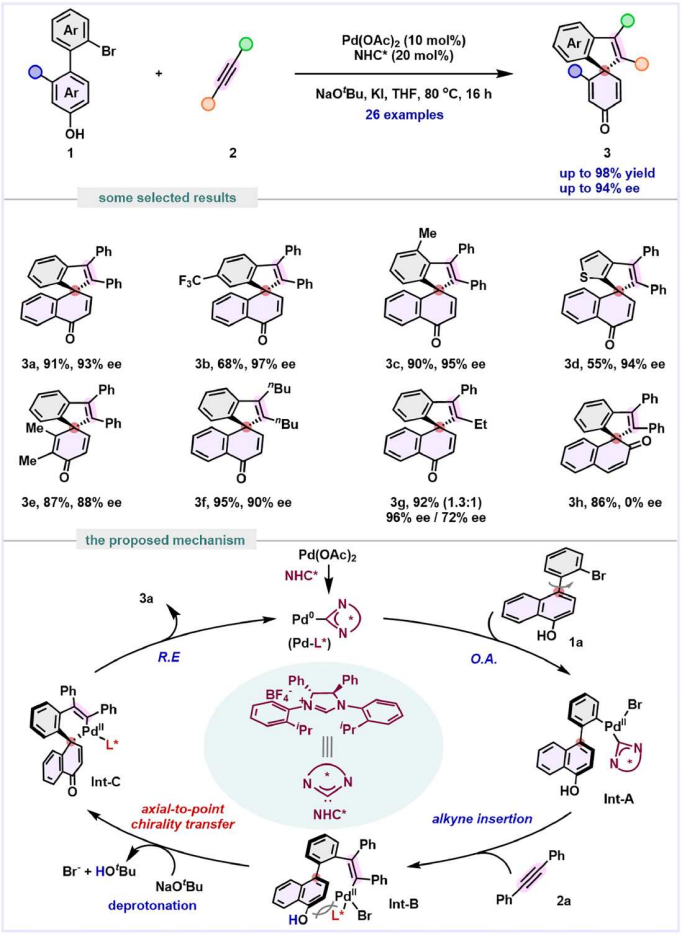

Figure 3 (Color online) DYKAT of racemic biaryls: axial-to-central chirality transfer.

2.2 Via reductive elimination

Notably, You *et al.* [24] reported the first Rh-catalyzed asymmetric naphthol dearomatization reaction initiated by $C(sp^2)$–H functionalization in a back-to-back manner, breaking the limitation that traditional naphthol dearomatization relies on pre-functionalization [37–39] and providing an efficient pathway for the synthesis of chiral spirocyclic compounds (Figure 4). Using chiral Cp*Rh complex (**Cp*Rh 1**) as the catalyst, $Cu(OAc)_2$/air as the oxidation system, K_2CO_3 as the base, and toluene as the solvent, the reaction achieves the cyclization of 1-aryl-2-naphthols **4** with internal alkynes **5** at 85 °C, efficiently synthesizing chiral spirocyclic enones **6** bearing an all-carbon quaternary stereocenter. The system features good substrate compatibility, affording the products in up to 98% yield, 94% ee, and 17:1 rr.

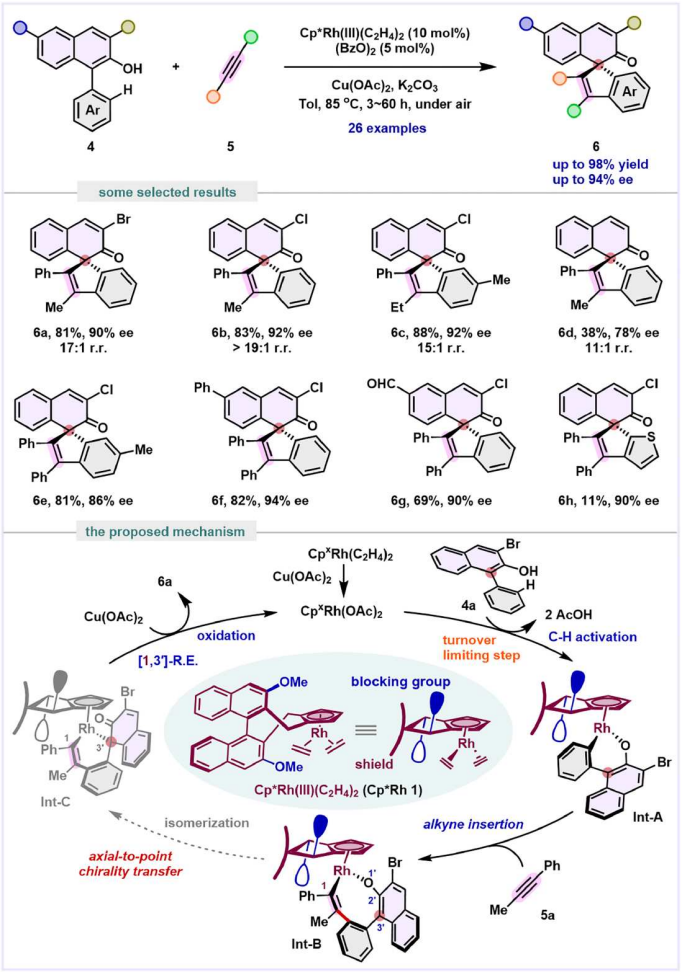

Figure 4 (Color online) Enantioselective dearomatization of naphthols via a Rh-catalyzed C(sp^2)–H functionalization/annulation.

DFT calculations [40] have made key revisions to the originally proposed reaction mechanism and provided in-depth mechanistic insights, proposing a refined catalytic cycle: (1) the reaction starts with the O–H deprotonation and C–H activation of naphthol **4a** The latter proceeds via the concerted metalation-deprotonation (CMD) mechanism, which is confirmed as the rate-determining step, and the acetic acid generated by the neutralization of K_2CO_3 renders this step irreversible; (2) after alkyne **5a** coordination, migratory insertion occurs to form an eight-membered rhodacyclic intermediate Int-B. This step is the enantioselectivity- and regioselectivity-determining step, revising the original hypothesis of the Rh-enolate intermediate—the product is directly generated from the eight-membered ring intermediate Int-B via [1,3′]-reductive elimination; (3) the Rh(I) product is oxidized to regenerate Rh(III) by $Cu(OAc)_2$, completing the catalytic cycle. In addition, DFT calculations have revealed that the six-membered rhodacyclic intermediate generated after C–H activation exists in four diastereomers, but they can rapidly racemize. Thus, the C–H activation step makes no significant contribution to asymmetric induction, further confirming that alkyne insertion is the core control step for stereoselectivity.

Subsequently, Lam and co-workers [41] reported a similar Rh-catalyzed asymmetric C(sp^2)–H functionalization/oxidative spiroannulation reaction, providing an efficient pathway for the synthesis of chiral spiroindenes containing all-carbon quaternary stereocenters (Figure 5) [42–44]. The reaction uses α-aryl cyclic 1,3-dicarbonyl compounds (or their enol tautomers) **7** and internal

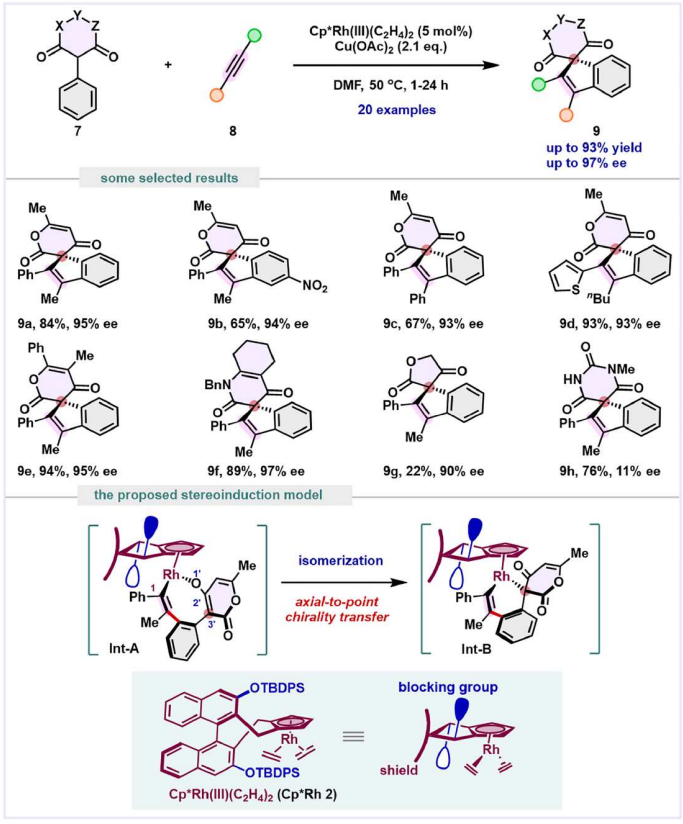

Figure 5 (Color online) Enol-directed Rh-catalyzed C–H functionalization and spiroannulation.

alkynes **8** as substrates. The core innovation lies in the successful regulation of the selectivity between the two potential directing groups in the substrate, prioritizing cyclorhodation via enol direction. The optimal catalytic system consists of the chiral Cp*Rh complex (**Cp*Rh 2**) as the catalyst, $Cu(OAc)_2$ as the oxidant, and *N*,*N*-dimethylformamide (DMF) as the solvent, proceeding efficiently at 50 °C without additional additives. The reaction exhibits excellent stereoselectivity, with enantioselectivity up to 97% ee and regioselectivity up to 19:1 rr. In contrast to the work of You's group [24], they proposed that the high selectivity between the two potential enol directing groups and the control over the rotation direction during the isomerization of O-bound rhodium enolate Int-A to the C-bound isomer Int-B are the key to achieving high enantiomeric excess values.

In comparison, the Pd/NBE cooperative catalysis system developed by Cheng and co-workers [45] expands the scope of this strategy from all-carbon quaternary stereocenters to P(V)-stereogenic centers in 2024 (Figure 6), and achieves enantiodivergent synthesis through solvent regulation, which is a major breakthrough in the diversification of chiral element construction. They innovatively combined the Catellani reaction [46–50] with axial-to-central chirality transfer and proposed a solvent-regulated stereoselectivity strategy: using prochiral aromatic iodides **10** and N-aryl/alkyl phosphonamides **11** as substrates, two P(V) enantiomers **12** can be selectively generated with a single chiral norbornene (**NBE***, **N1**) catalyst by adjusting solvent polarity.

Systematic optimization identified the core reaction conditions: with $Pd(OAc)_2$ as the catalyst precursor and tri(2-furyl)phosphine (TFP)/NBE* as the ligands, the (R_p)-configured product is mainly formed in the nonpolar solvent toluene (with ^{t}BuONa as the base), while the (S_p)-configured product is predominantly obtained in the polar solvent acetonitrile (with K_2CO_3 as the base). This system

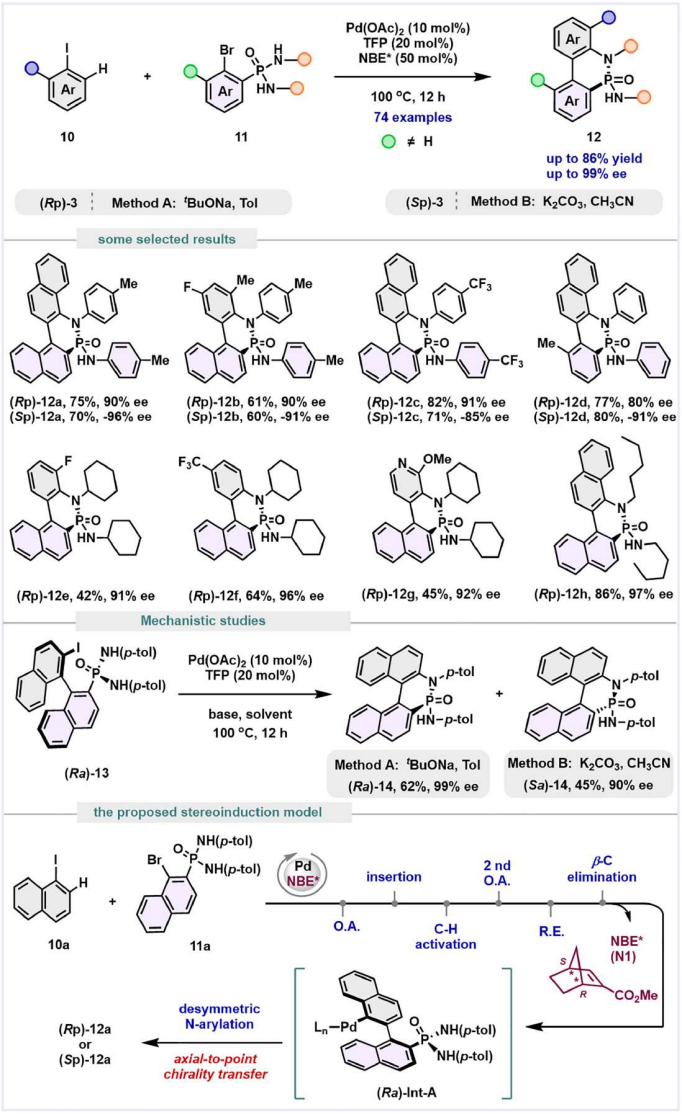

Figure 6 (Color online) Solvent-controlled enantiodivergent construction of P(V)-stereogenic molecules via Pd-catalyzed annulation.

exhibits broad substrate compatibility: aromatic iodides include *ortho*-, *meta*-, *para*-substituted, heterocyclic (pyridine), and polycyclic (naphthalene) derivatives; phosphonamides are compatible with functional groups such as methyl, halogens, and trifluoromethyl; N-alkyl phosphonamides can also react efficiently with a slight temperature increase to 105 °C, with enantiomeric excess values of up to 99%. It should be noted that aryl iodides without *ortho*-substituents cannot form the target product due to the "ortho effect".

Mechanistic studies confirmed that the reaction proceeds through an axial chirality to P(V) central chirality transfer process: under Pd catalysis, **10a** and **11a** form axially chiral intermediates Int-A with chiral **NBE**. Solvent polarity regulates the stereoselectivity of intramolecular N-arylation by influencing the conformation of the intermediates—nonpolar solvents stabilize one conformation leading to the (R_p)-product, while polar solvents favor the (S_p)-product. Control experiments further verified: phosphonamide substrates **13** with smaller steric hindrance result in a significant decrease in ee values; axially chiral substrates can directionally generate P(V) products **14** of the corresponding configuration in different solvents, confirming the decisive role of solvents in the direction of stereogenic transfer.

2.3 Via alkene insertion

In 2020, Zhang and co-workers [51] developed a palladium-catalyzed intermolecular dynamic kinetic asymmetric dearomatization reaction of 3-arylindoles **15** with internal alkynes **16** (Figure 7). The unique strategy of using a chiral sulfinamide phosphine ligand (**Sadphos**) [52–60] and achiral **Xantphos** as co-ligands provides a new idea for stereoselectivity control and an efficient pathway for the synthesis of chiral spiro[indene-1,3′-indole] compounds **17** bearing an all-carbon quaternary stereocenter. The reaction employs Pd(**Xantphos**)Cl_2 as the catalyst precursor, Sadphos as the chiral ligand, K_2CO_3 as the base, and toluene as the solvent, proceeding at 70 °C for 72 h. The product yield reaches a maximum of 92%, with an enantiomeric excess up to 98% ee.

In terms of substrate compatibility, the reaction exhibits broad applicability. 3-Arylindole substrates tolerate various substitution patterns: electron-donating groups such as methyl and methoxy, as well as electron-withdrawing groups such as chlorine and fluorine on the indole ring, don't affect the reaction, and different substituents on the 2-bromophenyl group are also well tolerated. Internal alkyne substrates cover symmetric aryl alkynes, heterocyclic alkynes (di(thiophen-2-yl)acetylene), dialkyl alkynes (4-octyne, 5-decyne), and functionalized alkynes (ester-, vinyl-, silyl-substituted alkynes). The regioselectivity of reactions involving unsymmetrical internal alkynes is generally moderate.

Mechanistic studies indicate that Pd(**Xantphos**)Cl_2 and **Sadphos** *in situ* generate a ligand-hybridized Pd(0) active species Int-A, which has been confirmed by sonic spray electrospray ionization mass spectrometry (SAESI-MS) [61] and phosphorous-31 nuclear magnetic resonance (^{31}P NMR) spectroscopy. As the core of chiral induction, **Sadphos** dictates the stereochemistry during the alkyne

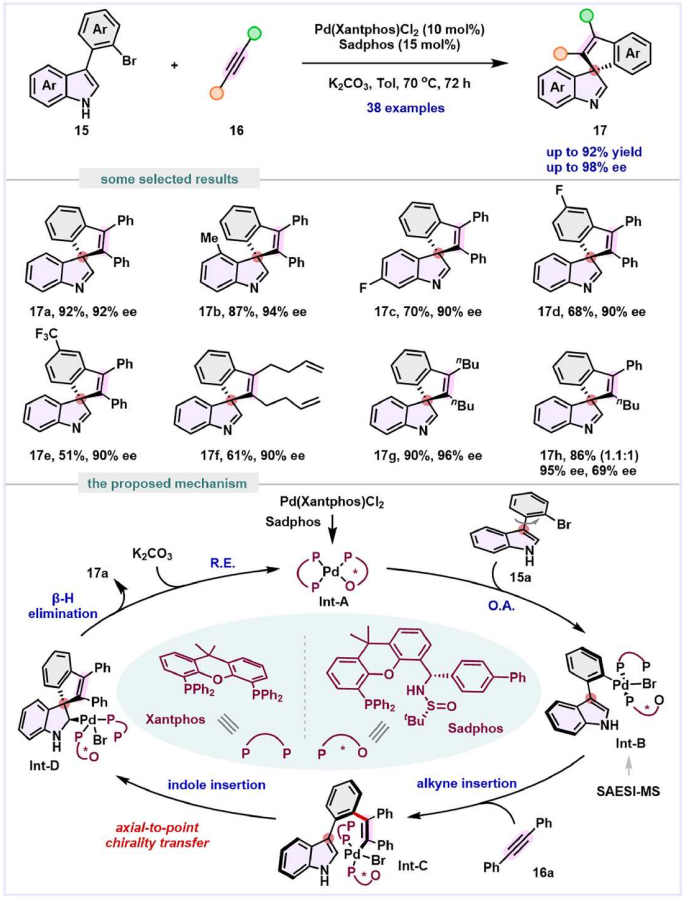

Figure 7 (Color online) Asymmetric dearomatization of indole by Pd/Sadphos catalyzed dynamic kinetic transformation.

insertion step and dominates the enantioselectivity; **Xantphos**, as an auxiliary ligand, optimizes the electronic properties and steric hindrance of the intermediates. The two ligands synergistically achieve a balance between high activity and high selectivity. The catalytic cycle initiates with the oxidative addition of the active species Int-A to the C–Br bond of 3-arylindole **15a**, forming the intermediate Int-B. Subsequent migratory insertion of the internal alkyne **16a** into the Pd–C bond generates the axially chiral intermediate Int-C. Through the migratory insertion of indole, intermediate Int-D is formed, realizing the transfer of axial chirality to central chirality and the dearomatization of indole. Finally, via *β*-hydride elimination and base-promoted reductive elimination, the chiral spirocyclic product **17a** is generated and the Pd(0) catalyst is regenerated.

In 2022, Jiao's group [62] developed a Pd-catalyzed intermolecular asymmetric spiroannulation reaction, achieving efficient coupling of 2,3-disubstituted indoles **18** with internal alkynes **19** via dynamic kinetic resolution (DKR) to modularly construct a series of chiral C2-quaternary spiroindolines **20** (Figure 8). The reaction employs $Pd(dba)_2$ as the catalyst precursor, **Carreira ligand** [63] as the chiral ligand, MeOLi as the base, and toluene as the solvent, operating at 90 °C with broad substrate compatibility and excellent functional group tolerance. For indole substrates: those with electron-donating/withdrawing groups (such as fluoro, chloro, methoxy) at the 5-position, methyl, 4,5-methylenedioxy and other substituents at the 6-position, as well as fused-ring structures like naphthyl and benzofuran, are all tolerated. For alkyne substrates: they cover symmetrical diaryl alkynes, di(thiophen-2-yl)acetylene, dialkyl alkynes, and unsymmetrical alkyl/aryl alkynes; only sterically hindered *ortho*-methyl substituted substrates fail to afford the desired product.

Mechanistic studies combined with DFT calculations have clarified the reaction mechanism: the spiroannulation follows the DKR mechanism—enantiomers of the indole substrate racemize rapidly at high temperature, meeting the requirements of dynamic kinetic resolution, and unreacted substrates remain racemic. Firstly, Pd forms an active species with the chiral Carreira ligand, which then undergoes oxidative addition with the C–Br bond on the aryl ring of the indole substrate **18a** to generate the aryl-Pd(II) intermediate Int-A. Subsequently, alkyne **19a** migratory insertion occurs to form the axially chiral alkene-Pd(II) intermediate Int-B, a step verified by DFT as both the rate-determining and selectivity-determining step. Immediately afterward, migratory insertion involving dearomatization of the indole takes place to form the chiral intermediate Int-C. Finally, *β*-H elimination and base-promoted reductive elimination afford the target product **20a**, with the regeneration of Pd(0) species to complete the catalytic cycle.

In the same year, Xu and co-workers [64] first realized the catalytic chirality transfer of axially chiral styrene intermediates under Pd(II) catalysis (Figure 9). By integrating asymmetric C–H activation [65–67] with double carbopalladation, they constructed a [3+2] annulation reaction, which provides an efficient pathway for the synthesis of chiral indenes **23** and offers important insights for other chirality transfer reactions. The reaction uses $Pd(OAc)_2$ as the catalyst precursor, **Ac-L-Ala-OH** as the chiral ligand, and AgOAc as the oxidant, conducted in THF at 80 °C for 48 h.

The substrate compatibility is broad with excellent functional group tolerance, covering more than 30 substrate combinations. Oxime ether substrates are compatible with both cyclic (2-arylcyclohex-2-enone oxime ethers) and acyclic (2-naphthalenylacrylaldehyde oxime ethers) structures. Electron-donating groups (methyl, methoxy), electron-withdrawing groups (fluoro,

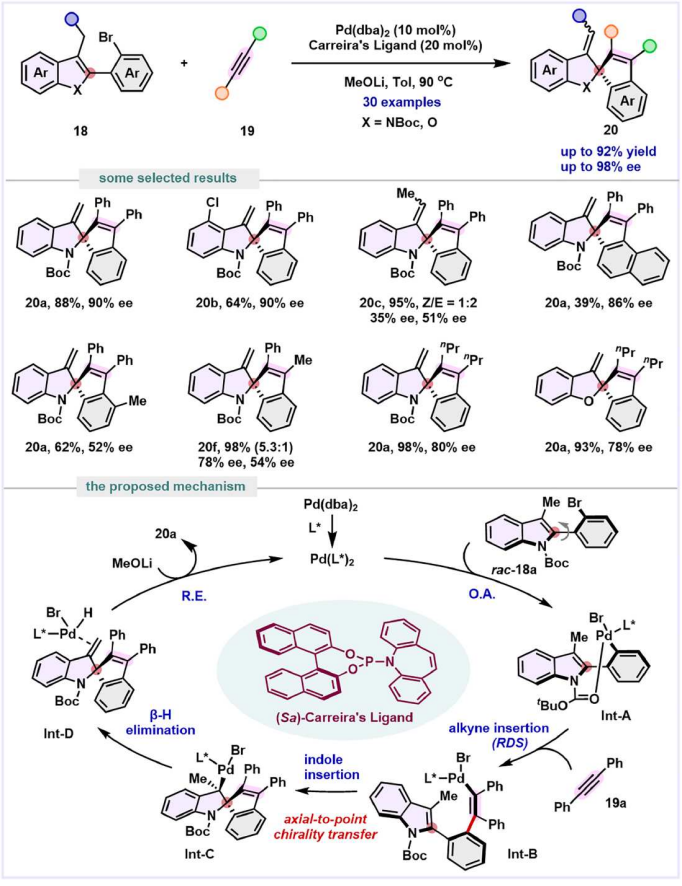

Figure 8 (Color online) Pd-catalyzed asymmetric spiroannulation reaction of C2-arylindoles with internal alkynes.

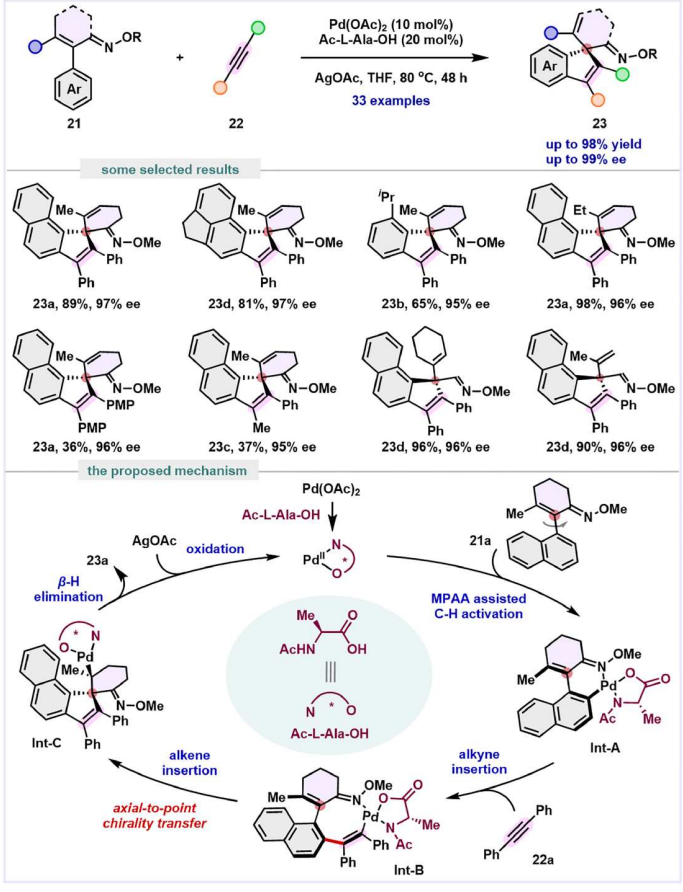

Figure 9 (Color online) Pd-catalyzed transient chirality transfer and atroposelective C–H functionalization.

chloro, trifluoromethyl), and polycyclic skeletons on the benzene ring are all tolerated. Acyclic oxime ethers yield nonspiro products with configurations opposite to those of spiro products. Alkyne substrates include symmetrical diaryl alkynes, naphthyl alkynes, and unsymmetrical arylalkyl alkynes. The steric hindrance from *ortho*-substituents has a negligible impact on the reaction, and unsymmetrical alkynes produce only a single regioisomer. The reaction yield reaches up to 98%, and the enantioselectivity peaks at over 99% ee.

Mechanistic studies indicate that the reaction initiates with oxime-directed asymmetric C–H activation to generate the axially chiral Pd(II) intermediate Int-A. Subsequently, alkyne **22a** coordination and migratory insertion form the axially chiral eight-membered palladacycle Int-B. Efficient axial-to-central chirality transfer is achieved through intramolecular alkene migratory insertion. Finally, the target product **23a** is formed via β-H elimination, and Pd(0) is oxidized by AgOAc to regenerate Pd(II), completing the catalytic cycle.

In 2016, Shibata's group [68] broke through the limitations of traditional cycloaddition reaction types of biphenylenes and first attempted an Ir-catalyzed asymmetric formal [4+1] cycloaddition of biphenylenes [69] with alkenes, tentatively synthesizing a chiral benzo[c]fluorene **26** bearing an all-carbon quaternary stereocenter with moderate enantioselectivity (Figure 10). Using $[Ir(cod)Cl]_2$ as the catalyst precursor, chiral ***xyl*-BINAP** as the ligand, benzo[a]-biphenylene **24** and styrene **25** as substrates, and xylene as the solvent, the reaction was carried out at 135 °C for 2 h, ultimately affording the target product in 89% yield with 55% ee.

Through mechanistic verification experiments and DFT studies [70], the authors proposed a plausible reaction mechanism, which achieves the transfer of transient axial chirality to central chirality under the regulation of the chiral ***xyl*-BINAP** ligand. The specific process is as follows: First, the Ir(I) catalyst undergoes oxidative addition to the sterically less hindered C–C bond of benzo[a]-biphenylene **24**, forming the dibenzoiridacyclopentadiene intermediate Int-A. At this point, the ***xyl*-BINAP** ligand has already coordinated with the Ir center, constructing a fixed chiral environment; subsequently, styrene **25** undergoes regioselective insertion into the Ir–C bond to form the seven-membered metallacyclic intermediate Int-B, and the spatial restriction of the chiral pocket allows the alkene to insert only from a single direction; then, β-hydrogen elimination occurs to generate the axially chiral Ir-hydride species Int-C, which is the key branch point that diverts the reaction from [4+2] cycloaddition to the [4+1] pathway; further, intramolecular alkene insertion takes place to form a five-membered ring intermediate, realizing the transfer of axial-to-central chirality; finally, reductive elimination generates the chiral product **26**, and the Ir(I) catalyst is regenerated to complete the catalytic cycle.

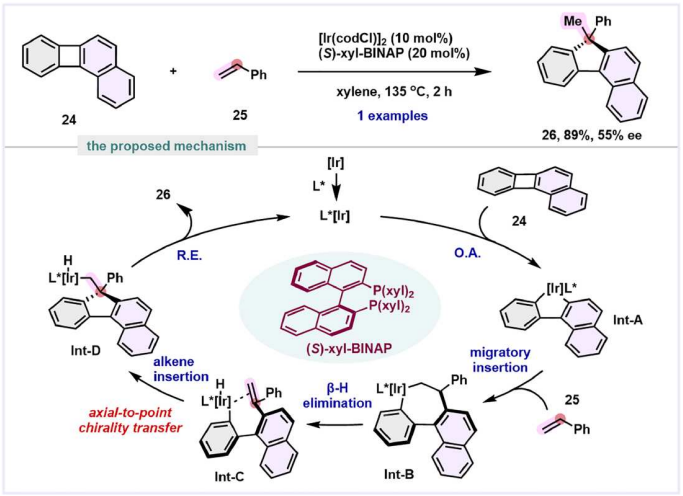

Figure 10 (Color online) Ir-catalyzed formal [4+1] cycloaddition of biphenylenes with alkenes initiated by C–C bond cleavage.

2.4 Via carbonyl insertion

In 2020, Zhou's group [71] established a new paradigm for the synthesis of chiral fluorenols through a palladium/chiral norbornene cooperative catalysis strategy, featuring a unique axial-to-central chirality transfer mechanism, which significantly breaks through traditional bottlenecks (Figure 11). The reaction employs $Pd(OAc)_2$ as the catalyst precursor, chiral norbornene [72–74] (**NBE***, **N2**) as the chiral cocatalyst, tri(2-furyl)phosphine (**TFP**) as the auxiliary ligand, K_2CO_3 as the base, and CH_3CN as the solvent, proceeding at 120 °C for 24–48 h. The **TFP** ligand can significantly enhance reaction activity, while **N2** provides precise stereinduction, maintaining extremely high stereoselectivity even under high-temperature conditions.

In terms of substrate compatibility, this strategy exhibits excellent versatility, expanded to 23 substrate combinations: Aryl iodides **27** have no strict restrictions, as electron-donating groups (methyl, methoxy), electron-withdrawing groups (fluoro, chloro, nitro), and heteroaryls all undergo efficient reactions; aryl bromides **28** must contain an *ortho*-carbonyl functional group (such as acetyl, ester, *etc.*) to provide a site for intramolecular migratory insertion, and substituents such as alkyl, cycloalkyl, and phenyl are compatible adjacent to the carbonyl group. The maximum reaction yield reaches 95%, and the maximum enantioselectivity is up to 99% ee, with extremely high stereochemical fidelity.

A clear and definite reaction mechanism is proposed. First, $Pd(OAc)_2$, together with chiral norbornene **N2**, aryl iodide **27d**,

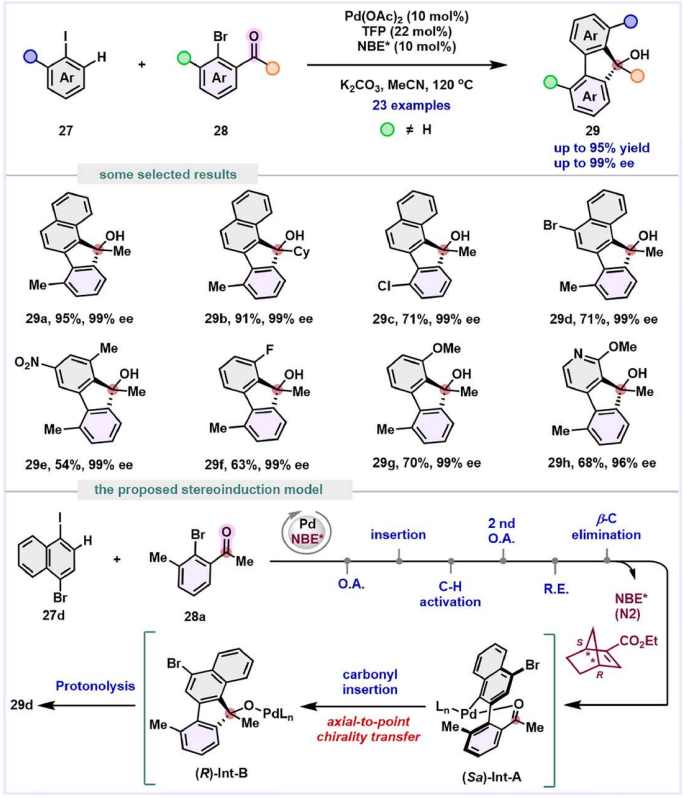

Figure 11 (Color online) Construction of chiral fluorenols through axial-to-central chirality transfer in high stereochemical fidelity.

and aryl bromide **28a**, sequentially undergoes oxidative addition, **NBE*** insertion, reductive elimination, and β-carbon elimination to form the axially chiral biaryl-Pd(II) complex Int-A; subsequently, the *ortho*-carbonyl group of the aryl bromide undergoes intramolecular migratory insertion with the Pd center to form the chiral intermediate Int-B, which is then converted to chiral fluorenol **29d** via protodepalladation.

In 2024, Zhou's group [75] innovatively combined Pd/**NBE*** cooperative catalysis with an enantioconvergent strategy (Figure 12). Without the need for external redox reagents, the strategy involves Pd(II)-initiated oxidation of secondary alcohols to generate ketone intermediates [76–78], followed by Pd(0)/**NBE***-catalyzed asymmetric Catellani-type cyclization, achieving efficient axial-to-central chirality transfer for the construction of chiral fluorenols. This strategy solves the problem of scarce asymmetric synthesis methods for chiral fluorenols through a redox-neutral process involving the destruction-reconstruction of stereogenic elements and provides important insights for the asymmetric transformation of racemic raw materials.

The reaction uses $Pd(OAc)_2$ as the catalyst precursor, 1,3-bis-(diphenylphosphino)propane (**DPPP**) and chiral norbornene (**NBE***, **N1**) as ligands, K_2CO_3 as the base, readily available aryl iodides **30** and racemic *ortho*-bromobenzyl alcohols **31** as raw materials, and 1,2-dichloroethane (DCE) as the solvent, proceeding at 110 °C. This system exhibits broad substrate compatibility, covering 49 substrate combinations. Aryl iodide substrates are compatible with alkyl, halogen, ester, amide and other functional groups at the *ortho*-, *meta*-, and *para*-positions; heteroaryl iodides and quinolinyl iodides can also react smoothly. Racemic secondary alcohol substrates can tolerate sterically hindered tert-butyl, fused-ring naphthyl, and heteroaryl substitutions, as well as electron-donating/withdrawing groups, with the enantiomeric excess values of the products stably maintained at 90%–99% ee.

The proposed catalytic cycle is as follows: first, Pd(II) oxidizes racemic secondary alcohols **31a** to generate *ortho*-bromoacetophenone **31a′** and Pd(0). Pd(0) undergoes oxidative addition, alkene insertion, and C–H activation with aryl iodides **30a** and **NBE*** to form the Pd(II) intermediate Int-A (ANP*). Subsequently, it undergoes oxidative addition with *ortho*-bromoacetophenone to form the Pd(IV) intermediate Int-B. Then, the reductive elimination step of *ortho*-C–H arylation (the stereoselectivity-determining step) forms the axially chiral intermediate Int-C, followed by β-C elimination to form the axially chiral intermediate Int-D. Intramolecular carbonyl insertion generates the chiral intermediate Int-E, and protonation yields the (*S*)-configured product **32a** and regenerates Pd(II), completing the catalytic cycle. DFT calculations have revealed the stereocontrol mechanism of the reaction: high enantioselectivity is achieved through axial-to-central chirality transfer. The key lies in the transition state regulation during the reductive elimination step —when the Pd(IV) intermediate Int-B undergoes reductive elimination, due to the steric hindrance effect of chiral **NBE***, only the transition state without repulsion reacts preferentially, forming the stable axially chiral intermediate Int-C.

In 2025, Song's group [79] developed a nickel-catalyzed regio- and enantioselective reductive [3+2] annulation reaction (Figure 13). Innovatively adopting environmentally friendly bis(pinacolato)-diboron (B_2pin_2) as the reducing agent [80–82], this reaction successfully overcomes traditional limitations through efficient axial-to-central chirality transfer, breaking the monopoly of precious metals (Pd, Rh, Ir) and providing a practical and efficient new catalytic system.

The reaction uses $NiBr_2$·dimethoxyethane ($NiBr_2$·DME) as the

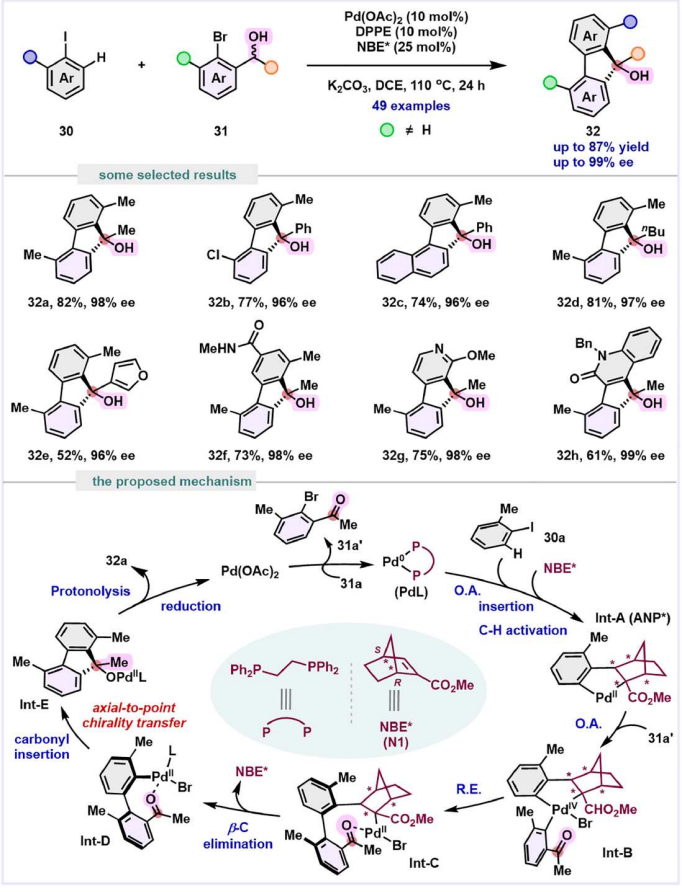

Figure 12 (Color online) Enantioconvergent synthesis of chiral fluorenols via redox-neutral Pd(II)/chiral norbornene cooperative catalysis.

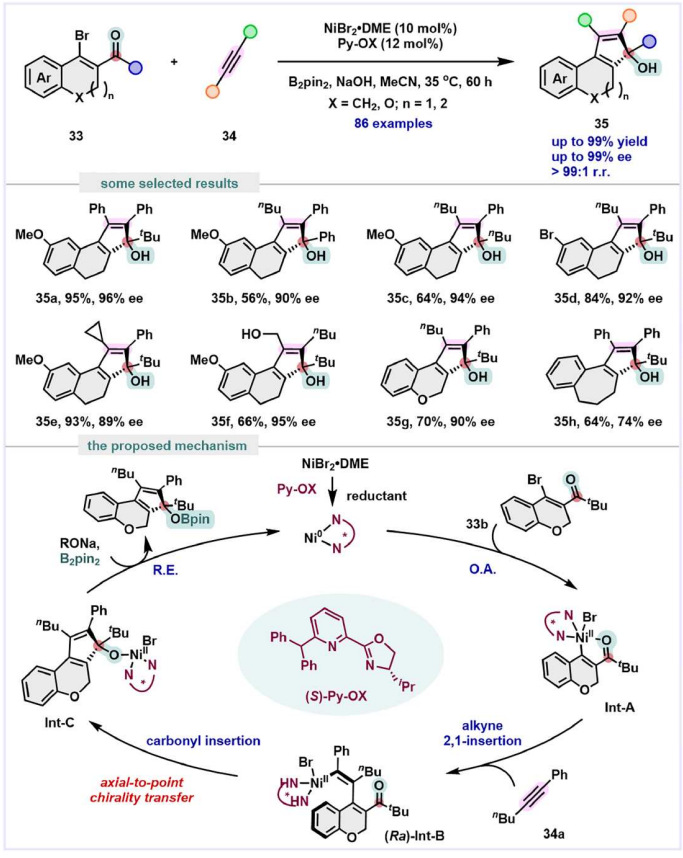

Figure 13 (Color online) Nickel-catalyzed regio- and enantioselective reductive [3+2] annulation of β-bromoenones with alkynes.

catalyst precursor, pyridine-oxazoline (**Py-OX**) as the chiral ligand, *β*-bromoenones **33** and alkynes **34** as raw materials, and CH_3CN as the solvent, proceeding at 35–60 °C. B_2pin_2 and NaOH synergistically achieve reductive cyclization, compatible with more than 80 substrate combinations. The product **35** exhibits a maximum isolated yield of 95% and enantioselectivity up to 96% ee, while the regioselectivity of unsymmetrical alkynes exceeds 99:1 rr. Alkyne substrates include symmetrical diaryl alkynes, heteroaryl alkynes, unsymmetrical arylalkyl alkynes, and 1,3-enynes, with ester, amide, halogen, and other functional groups all well tolerated. *β*-Bromoenone substrates support alkyl, aryl, and heteroaryl substitutions; even seven-membered ring skeletons can react efficiently, with only a slight decrease in yield for sterically hindered substrates.

Mechanistic studies combined with DFT calculations reveal the reaction essence: Ni(II) is first reduced to active Ni(0) species, which undergo oxidative addition with *β*-bromoenones **33b** to form intermediate Int-A. Subsequently, alkynes **34a** undergo regioselective migratory insertion to form axially chiral intermediate (R_a)-Int-B, followed by intramolecular carbonyl insertion to achieve chirality transfer, generating intermediate Int-C. Finally, the target product **35g** is obtained through transmetallation and reductive elimination. Regioselectivity is determined by the migratory insertion mode of alkynes, with unsymmetrical alkynes preferentially undergoing 2,1-insertion. The spatial interactions between the chiral ligand **Py-OX** and the substrate, together with weak C–H···O bonds, collectively regulate the preferred configuration.

2.5 Other types

2.5.1 *Via imine insertion*

In 2022, Jia's group [83] developed a cobalt-catalyzed enantioselective dearomative [3+2] umpolung annulation of N-heteroarenes with alkynes, providing an efficient protocol for the synthesis of chiral N-heterocyclic compounds bearing spiro quaternary stereocenters [84–86] (Figure 14). This method breaks through the limitations of traditional synthesis that depends on preactivated substrates or nucleophilic organometallic reagents, directly utilizing non-preactivated N-heteroarenes [87,88]. Through the synergistic effect of cobalt catalysis and a reducing agent, it achieves efficient transformation of 7 substrates under mild conditions, with enantioselectivity up to 97% ee.

The reaction system uses CoI_2 as the catalyst precursor, (*S*)-**^{i}Pr-PHOX** as the chiral ligand, zinc powder as the reducing agent, 2-arylisoquinolines (or 2-arylquinolines) **36** and 2-butyne **37** as substrates. The reaction is conducted in 1,2-dimethoxyethane (DME) at 60 °C for 48 h, followed by oxidation with H_2O_2 to convert the unstable cycloadduct into stable derivatives **38**.

Based on literature reports [89], a tentative mechanism was proposed. The reaction initiates with the reduction of Co(II) to active Co(I) species by zinc powder. Subsequently, Co(I) undergoes oxidative addition with the aryl bromide of N-heteroarenes **36d** to form the aryl-cobalt(III) intermediate Int-A. After alkynes **37** undergo migratory insertion to form the axially chiral vinyl-cobalt (III) intermediate Int-B, it undergoes intramolecular dearomative migratory insertion with the C=N bond of N-heteroarenes to construct the spiro quaternary stereocenter. Finally, protonation with isopropanol generates the unstable product, which is oxidized to the stable product **38** by hydrogen peroxide. Meanwhile, Co(III) is reduced back to Co(I) by zinc, completing the catalytic cycle.

2.5.2 *Via nucleophilic attack*

In 2025, Liu's group [90] first reported a Pd-catalyzed formal [3+1+1] spiroannulation reaction, enabling the efficient synthesis of

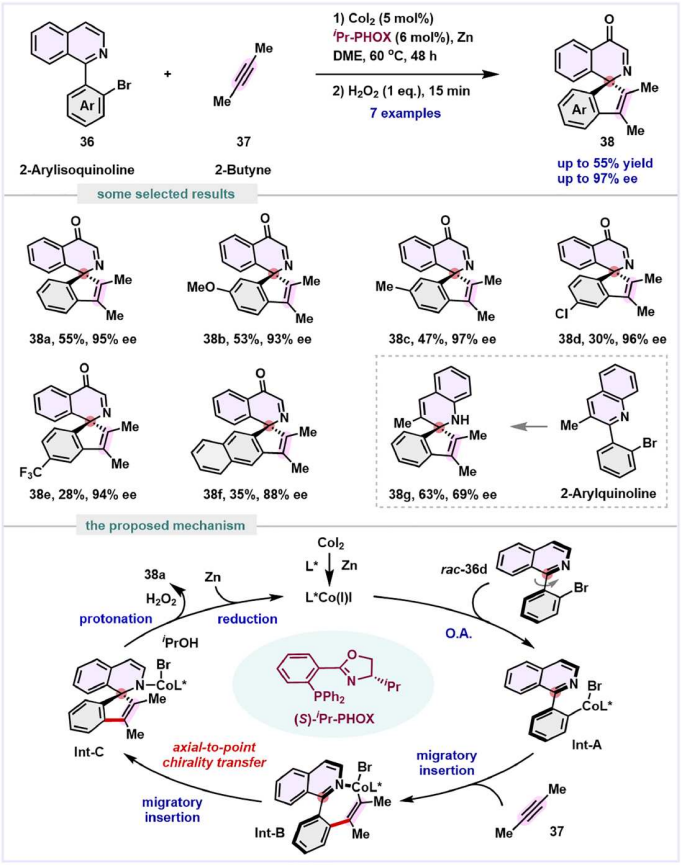

Figure 14 (Color online) Cobalt-catalyzed enantioselective dearomative [3+2] umpolung annulation of N-heteroarenes with alkynes.

chiral (N,N)-spiroketals [91–94] from racemic quinazoline-derived heterobiaryl triflates **39**, carbon monoxide (CO) **40**, and amines **41** through a cascade process of enantioconvergent aminocarbonylation and intramolecular dearomative nucleophilic aza-addition (Figure 15). This reaction is compatible with more than 80 substrates, achieving a maximum yield of 99% and enantioselectivity up to 98% ee. It fills the structural gap in the synthesis of spirocyclic compounds, expands their application in chiral ligand design, and provides valuable insights for the synthesis of similar scarce skeletons.

Two core reaction systems were optimized: for alkylamine substrates, $Pd(acac)_2$ was used as the catalyst precursor, **JOSIPHOS**-type ligand as the chiral ligand, and the reaction was conducted in DME at 50 °C; for arylamine substrates, $Pd(OAc)_2$ served as the catalyst precursor, bisphosphine ligand **QuinoxP*** or **BenzP*** as the chiral ligand, and the reaction proceeded in a mixed solvent of DCM/DCE at 80 °C. Both systems require a 10 atm CO atmosphere. A prominent advantage of this method is its broad substrate compatibility, covering over 80 substrate combinations. Amine substrates include alkylamines, arylamines, and amines derived from drug fragments, with ether bonds, thioethers, ester groups, heterocycles, and other functional groups all well tolerated. Among heterobiaryl triflate substrates, electron-donating/withdrawing substituents (such as methyl, fluoro, cyano) on the quinazoline ring and naphthyl ring are compatible, while only substrates with anisole replacing the naphthyl ring are inactive. The products **42** exhibit a maximum yield of 99% and the highest ee value of 98%. The practical value of this method lies in its multiple derivatization potentials. Products can be converted into thio-derivatives via oxygen-sulfur exchange reactions, or into chiral quaternary ammonium salts as carbene ligand precursors. More

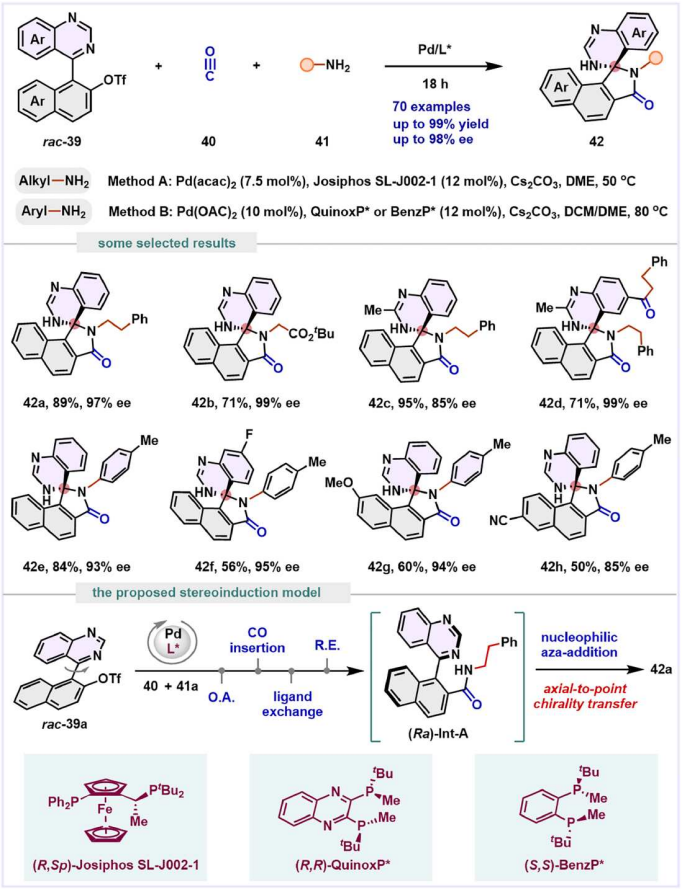

Figure 15 (Color online) Catalytic asymmetric synthesis of (N,N)-spiroketal via Pd-catalyzed enantioconvergent aminocarbonylation and dearomative nucleophilic aza-addition.

importantly, these ligand precursors successfully coordinate with transition metals such as Rh, Ir, Au, and Pd to form metal complexes, whose structures have been confirmed by X-ray crystallography.

Mechanistic studies indicate that the enantioselectivity of the reaction is determined by the aminocarbonylation step dominated by DYKAT, rather than the subsequent spiroannulation process. The Pd catalyst undergoes oxidative addition, CO insertion, ligand exchange, and reductive elimination with racemic substrates to generate the stable axially chiral amide intermediate (*Ra*)-Int-A. Subsequently, axial-to-central chirality transfer is achieved through intramolecular dearomative nucleophilic aza-addition. Control experiments confirm that substrates unable to form axially chiral intermediates yield products with 0% ee, directly verifying the chirality transfer mechanism.

Transition-metal-catalyzed dearomatization of phenols is an important method for the synthesis of spirocyclic compounds. However, intermolecular dearomatization reactions involving dienes have long remained underdeveloped due to their tendency to undergo *β*-hydride elimination, leading to the formation of Heck byproducts. In 2016, Luan's group [95] attempted a Pd(0)-catalyzed asymmetric dearomatization reaction of phenol-based biaryls **43** with 1,3-dienes **44**, preliminarily achieving the stereocontrolled synthesis of spirocyclohexadienone compounds bearing two contiguous tertiary/quaternary carbon centers (Figure 16).

The reaction uses $Pd(OAc)_2$ as the catalyst precursor, commercially available chiral phosphoramidite as the ligand, K_2CO_3 as the base, and DME as the solvent. When the unsaturated naphthol

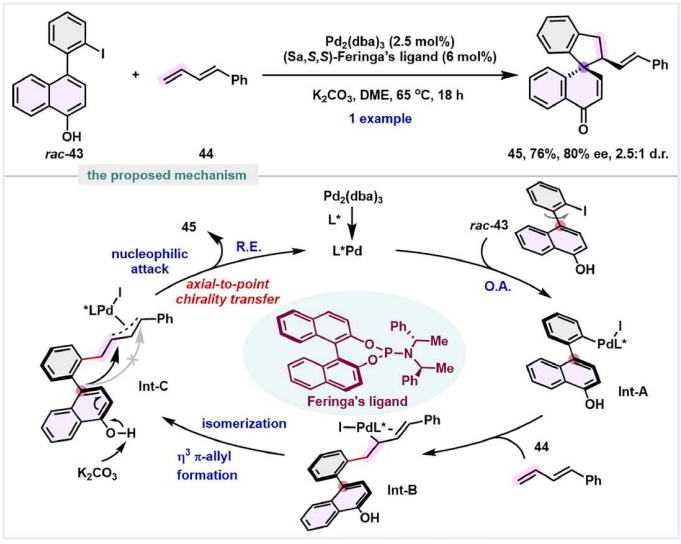

Figure 16 (Color online) Pd-catalyzed dearomative [3+2] spiroannulation of phenol-based biaryls with 1,3-dienes.

substrate **43** reacts with 1,3-diene **44**, the product **45** is obtained as a diastereomeric mixture (2.5:1 dr) with 76% yield and 80% ee for the major diastereomer, verifying the feasibility of asymmetric control.

The key steps of the Heck/Tsuji-Trost reaction mechanism [96] are as follows: (1) $Pd(OAc)_2$ is *in situ* converted to active Pd(0) species under the action of the ligand and base; (2) Pd(0) undergoes oxidative addition to the C–I bond of the phenol-based biaryl **43**, forming a Pd(II) intermediate; (3) the 1,3-diene **44** undergoes regioselective insertion into the Pd–C bond and isomerizes to form an axially chiral π-allyl-Pd intermediate Int-C; (4) the phenolic hydroxyl group is deprotonated by K_2CO_3, and the phenoxide acts as a nucleophile to selectively attack a single enantiotopic face of the π-allyl group, realizing the transfer of axial-to-central chirality; (5) the chiral spirocyclic product **45** is generated via reductive elimination, and Pd(0) is regenerated to complete the catalytic cycle.

2.5.3 *Via oxidation*

Traditional Rh(III)-catalyzed asymmetric spirocyclization reactions are limited to alkyne-based coupling partners, restricting the substrate scope [97,98]. The Rh(III)-catalyzed asymmetric spirocyclization reaction reported by Li's group [99] in 2020, through the innovative integration of C–H activation and axial-to-central chirality transfer, provides an efficient pathway for the synthesis of spirocyclic nitrones bearing an all-carbon quaternary center (Figure 17). It breaks through the substrate limitations of traditional spirocyclization reactions and offers a new idea for the construction of chiral spirocycles.

This study follows a chirality transfer cascade of C–H activation—formation of a transient axially chiral biaryl—oxidative cyclization. The reaction uses Cramer's chiral Cp*Rh(III) (**Cp*Rh 3**) as the catalyst, AgF_2 as the oxidant, pivalic acid (PivOH) and NaOAc as additives, and hexafluoroisopropanol (HFIP) as the solvent, proceeding at 0 °C for 24 h. Under this system, nitrones **46** undergo [1,4] cycloaddition with quinone diazides **47**, with the isolated yield of the product **48** reaching a maximum of 90% and an enantioselectivity peak of 97% ee.

The substrate compatibility exhibits broad applicability, covering more than 40 substrate combinations with different substitution patterns. Nitrone substrates can tolerate electron-donating groups (methyl, methoxy), electron-withdrawing groups (chloro, trifluor-

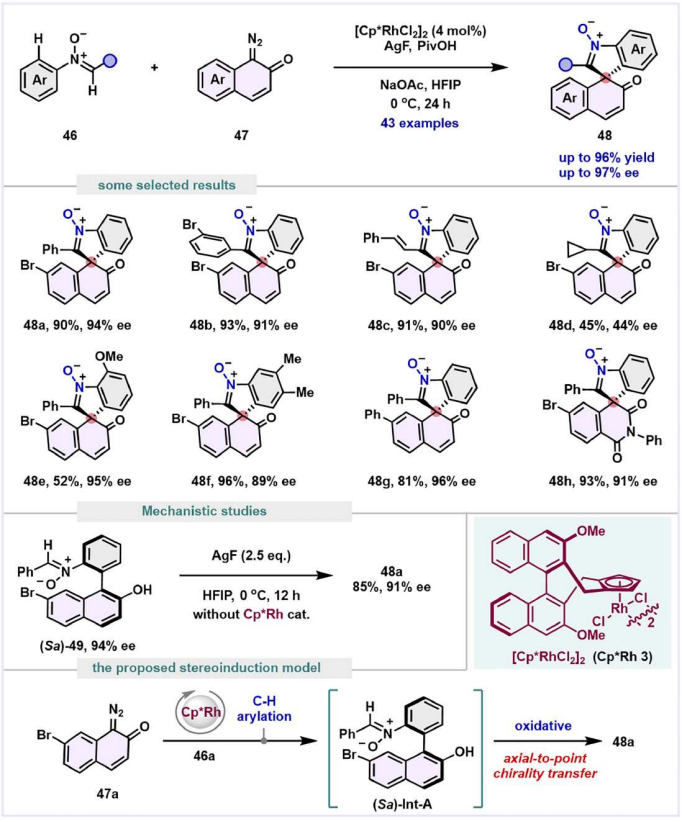

Figure 17 (Color online) Rh-catalyzed asymmetric spirocyclization via C–H activation and axial-to-central chirality transfer.

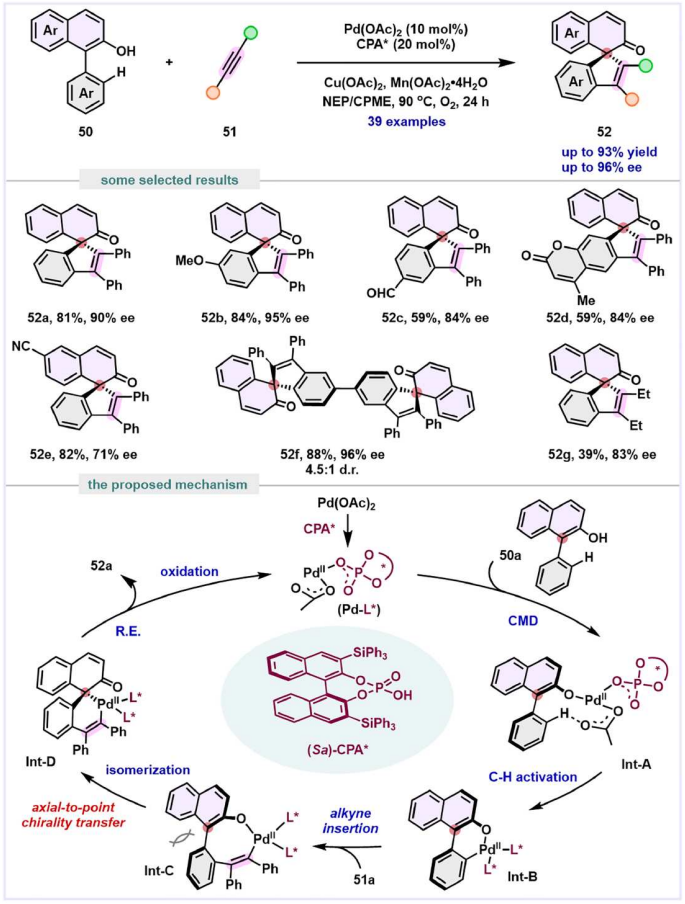

Figure 18 (Color online) Asymmetric C–H functionalization/dearomatization of naphthols via axial-to-central chirality transfer.

omethyl, ester), as well as heteroaryl (thiophene, benzofuran), naphthyl, alkenyl and other substituents; *ortho*-, *meta*-, and *para*-substitutions all undergo efficient reactions. Among quinone diazides, 7-substituted derivatives exhibit the best performance, and isoquinolinedione-based diazo compounds can also participate smoothly in the reaction. Only *para*-quinone diazides lead to product racemization due to the free rotation of the intermediate.

Mechanistic studies have revealed a unique chirality transfer pathway: the Rh(III) catalyst first undergoes C–H activation of the nitrone **46a** to form a rhodacyclic intermediate [100,101], which reacts with the quinone diazide **47a** to generate a transient axially chiral biaryl intermediate Int-A. Although this intermediate is thermodynamically unstable, it can be rapidly trapped through AgF_2-mediated single-electron oxidation, undergoing radical cyclization and secondary oxidation to complete dearomatization, and ultimately achieving efficient transfer of axial chirality to central chirality. Electron paramagnetic resonance (EPR) detection confirmed the existence of radical intermediates, and kinetic isotope effect studies indicated that C–H activation is not the rate-determining step, while the axial-to-central chirality transfer process is the rate-limiting step of the reaction.

2.5.4 *Via isomerization*

In 2025, Shi's group [102] reported a Pd(II)-catalyzed asymmetric C–H functionalization/dearomatization reaction of naphthols (Figure 18). Utilizing an axial-to-central chirality transfer strategy and commercially available chiral phosphoric acid (**CPA**) [103,104] as the ligand, this reaction efficiently synthesizes all-carbon chiral spirocycles. Conducted in a mixed solvent of NEP: CPME (1:9) under an O_2 atmosphere at 90 °C for 24 h, the reaction accommodates more than 30 types of substrates, achieving a maximum yield of 93% and enantioselectivity up to 96% ee.

For naphthol substrates, **50**: electron-donating groups (methyl, methoxy), electron-withdrawing groups (fluoro, cyano, ester groups) on the benzene ring, various substituents at the 6-position and 7-position of the naphthalene ring, as well as naphthols derived from the natural product Hymecromone and those with pharmaceutical skeletons, are all well tolerated. Notably, the product bearing two quaternary carbon stereocenters was obtained in 88% yield with 96% ee. Alkyne substrates **51** include symmetrical diaryl alkynes, dinaphthyl alkynes, and dialkyl alkynes; only unsymmetrical arylalkyl alkynes form a mixture of regioisomers. Notably, sterically hindered substituents (such as a phenyl group at the 6-position of the naphthalene ring) result in slight decreases in yield and ee value.

Mechanistic studies indicate that the reaction initiates through a concerted metalation-deprotonation (CMD) mechanism. Pd(II) acts synergistically with chiral phosphoric acid to form intermediate Int-A, which undergoes asymmetric C–H activation of naphthols **50a** to generate Pd(II) intermediate Int-B [105–107]. Subsequent ligand exchange and migratory insertion of alkynes **51a** form axially chiral intermediate Int-C. Driven by steric hindrance, rapid axial-to-central chirality transfer is achieved via isomerization to form intermediate Int-D, followed by reductive elimination to yield the product **52a**. Pd(0) is oxidized to Pd(II) by $Cu(OAc)_2/O_2$, completing the catalytic cycle. Deuteration experiments confirm that the cleavage of the C–H bond is irreversible, ruling out racemization caused by reversible protonation. The nonlinear relationship between the ee values of the ligand and the product suggests that multiple CPA ligand molecules participate in the enantioselectivity-determining step.

2.5.5 *Via C–H insertion*

Traditional asymmetric metal carbene reactions rely on a central-to-central chirality transfer mode, where neutral rhodium complexes tend to dissociate to form free intermediates, leading to reduced stereoselectivity [108]. In 2020, Xu's group [109] reported a transient axial-to-central chirality transfer strategy that achieves efficient synthesis of chiral fluorenes via rhodium-catalyzed carbene C(sp^2)–H functionalization [110–112] (Figure 19), which achieves the efficient synthesis of chiral fluorenes bearing tertiary carbon stereocenters. Notably, this work established a fundamental mechanistic framework and design principles for the subsequent development of catalytic systems targeting the construction of quaternary carbon stereocenters via C–H insertion.

The reaction employs Rh_2(**S-TFPTTL**)$_4$ as the catalyst, tert-butyl methyl ether (TBME) as the solvent, and 4 Å molecular sieves as the additive. The catalyst must be slowly added via a syringe pump over 40 min to ensure high enantioselectivity. Two general reaction modes were developed: (A) direct asymmetric C–H functionalization is suitable for stable diaryl diazo compounds **53**/**55**, compatible with diazo compounds containing electron-donating/withdrawing groups, heteroaryls, and naphthyl groups. (B) The carbene/alkyne metathesis (CAM) cascade reaction generates carbene intermediates *in situ*, solving the problem of difficult access and instability of donor-donor-type carbene precursors. It can tolerate aryl/alkyl alkynes, ester groups, trifluoromethyl groups, and other functional groups.

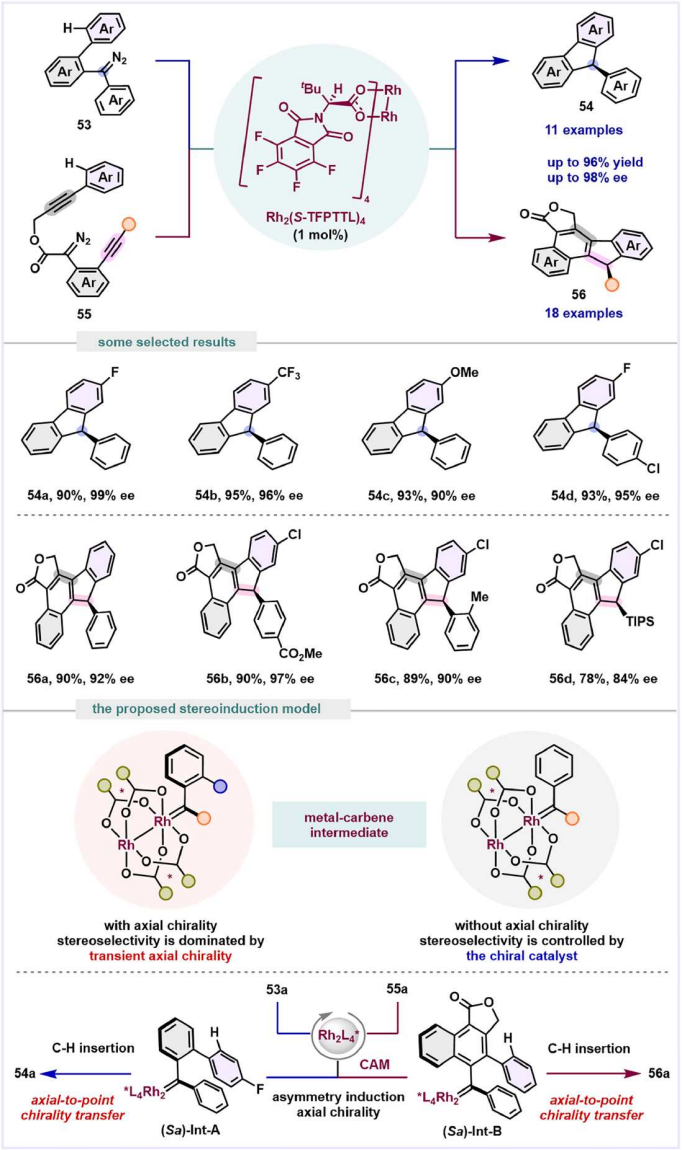

Figure 19 (Color online) Transient-axial-chirality controlled asymmetric Rh-carbene C–H functionalization.

3 Catalytic enantioselective synthesis via transient axial-to-axial chirality transfer

The research on transient axial-to-axial chirality transfer constitutes a significant extension of axial chirality transfer strategies, sharing the fundamental core principle with axial-to-central chirality transfer: chiral catalysts induce the *in situ* generation of transient C–C axially chiral intermediates, and prior to the racemization of these intermediates, chiral information is transferred to new axially chiral moieties with high fidelity. Notably, the regulatory logic governing transient axially chiral intermediates in such transformations is highly congruent with that in axial-to-central chirality transfer reactions. Consequently, the research advancements in this domain are poised to offer critical theoretical guidance and valuable methodological references for the development of novel axial chirality transfer systems.

3.1 Via reductive elimination

Due to the high rotational freedom and low rotational barrier of the C–N bond, the configurational stability of C–N axially chiral compounds is significantly lower than that of well-established C–C axially chiral counterparts [113–115]. In 2021, Zhou and co-workers [116] reported the first Pd/NBE*-catalyzed axial-to-axial chirality transfer strategy, breaking through the configurational stability bottleneck in the synthesis of C–N axially chiral compounds (Figure 20). Their mechanistic studies not only clarified the stereocontrol rules of chirality transfer but also provided theoretical guidance for the application of axial-to-axial chirality transfer in asymmetric catalysis, holding significant reference value for fields such as medicinal chemistry and chiral ligand synthesis. They innovatively proposed a high-fidelity transfer strategy of transient C–C axial chirality to C–N axial chirality: using aryl iodides **57** (with various substitution patterns including monocyclic, bicyclic, and heterocyclic) as substrates, and 2,6-disubstituted aryl bromides **58** containing amide groups as dual-function reagents (arylation & terminating reagent), a multi-step cascade reaction was realized under the synergistic effect of $Pd(OAc)_2$ (5 mol%), chiral NBE ((1*S*,4*R*)-2-ethylester-substituted norbornene, **N3**)/**TFP** ligand, and K_2CO_3 base.

The optimal reaction conditions were determined through systematic optimization: the reaction was conducted in CH_3CN or DMF at 70 °C for 45–72 h, avoiding racemization caused by high

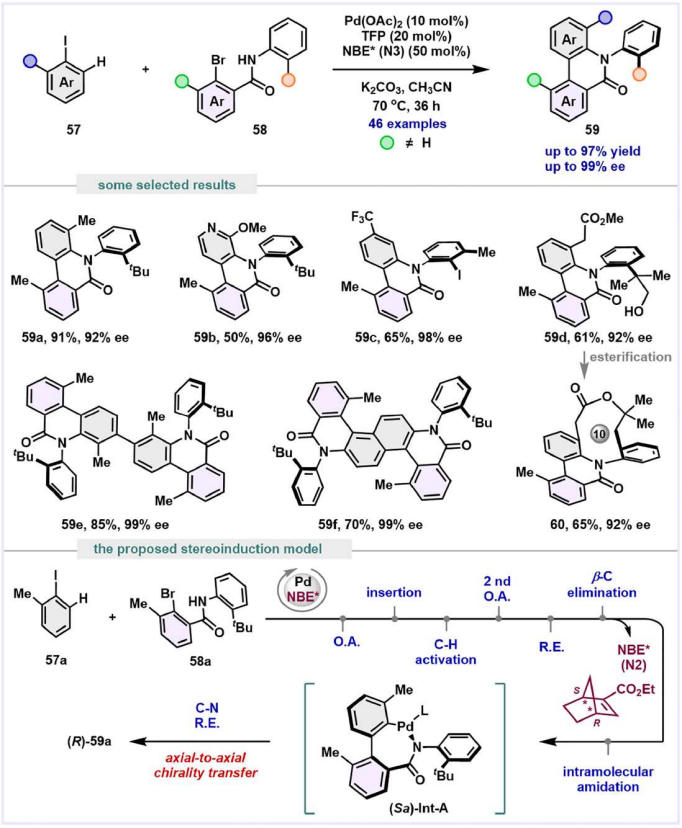

Figure 20 (Color online) Axial-to-axial chirality transfer strategy for atroposelective construction of C–N axial chirality.

temperatures. This system exhibited exceptional substrate compatibility, successfully synthesizing 46 types of C–N axially chiral phenanthridinones **59** with yields up to 97% and enantioselectivities up to 99% ee. Among them, heteroaryl iodides and polycyclic aryl iodides all reacted efficiently, and the aniline moiety of aryl bromides could tolerate various functional groups such as alkyl, halogens, and aldehydes. A key finding was that bulky aniline substituents are critical for the fidelity of chirality transfer (the ee of substrates with small steric hindrance was nearly 0), while *meta*-substitution of aryl iodides could enhance the stability of the C–N axis by reducing ground-state distortion. The rotational barrier, verified by both experiments and DFT calculations, was highly consistent, and no configurational racemization occurred below 70 °C. The products can be converted into macrocyclic products via macrolactonization.

DFT calculations clarified the reaction mechanism and the essence of chiral control: the catalytic cycle initiates with the oxidative addition of Pd(0) to aryl iodide **57a**, followed by NBE* insertion and *ortho* C–H activation to form an aryl/NBE* palladacycle intermediate. Subsequent secondary oxidative addition with aryl bromide **58a** generates a Pd(IV) species; C–C reductive elimination is the rate-determining step, forming an (S_a)-configured C–C axially chiral intermediate Int-A. Finally, the chirality is transferred to the (*R*)-configured C–N axially chiral product through irreversible intramolecular amidation.

Furthermore, Zhou and co-workers [117] achieved the first breakthrough in the asymmetric alkenyl Catellani reaction-breaking the traditional reaction's reliance on (hetero)aromatic substrates and overcoming the core issue of the low configurational stability of C–N axial chirality (Figure 21). Its axial-to-axial chirality transfer mechanism provides a new paradigm for the synthesis of complex chiral heterocyclic compounds, enriching the mechanistic

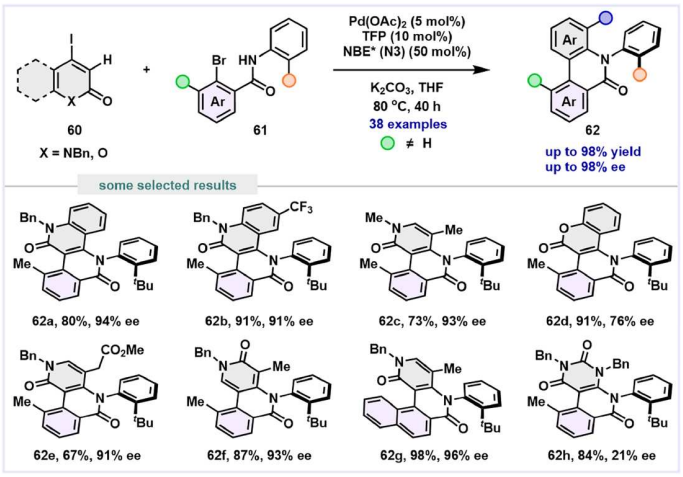

Figure 21 (Color online) Asymmetric alkenyl catellani reaction for the construction of C–N axial chirality.

connotations of asymmetric catalysis and axial chirality chemistry. They used partially aromatic iodinated 2-pyridones, quinolones, coumarins, and uracils as alkenyl iodide substrates **60**, which reacted with 2,6-disubstituted aryl bromides containing a tethered amide group. The optimal conditions were determined as follows: $Pd(OAc)_2$ (5 mol%) as the catalyst precursor, (1*S*,4*R*)-ethyl norbornene-2-carboxylate (**N3**, 50 mol%) as the chiral mediator, K_2CO_3 as the base, THF as the solvent, and the reaction was conducted at 80 °C for 48 h. Experimental results showed that the reaction is compatible with substrates bearing various electronic effects and steric hindrances, successfully preparing 38 types of polycyclic C–N axially chiral products with yields of up to 98% and enantioselectivities of up to 97% ee.

3.2 Via electrophilic attack

Aromatic chlorination represents a pivotal transformation in synthetic chemistry. Conventional approaches focus on the preparation of planar chloroarenes, while research on constructing three-dimensional molecules via chlorinative dearomatization remains underdeveloped [118–120]. In 2025, Luan's group [121] reported a dearomatization-rearomatization (DA/RA) tandem strategy (axial-to-axial-to-axial chirality transfer), which achieves efficient full resolution of these compounds through the synergistic effect of stereoselective chlorination and dechlorination, providing a novel paradigm for the synthesis of $C(sp^2)$–$C(sp^3)$ axially chiral molecules (Figure 22). This study not only broke through the limitations of traditional axial chirality resolution, realizing full resolution with high selectivity and broad applicability, but also enriched the connotation of asymmetric dearomatization chemistry through the closed-loop design concept of chirality storage-transfer.

The stereoselective chlorination serves as the kinetic resolution. Using $Sc(OTf)_3$ as the catalyst precursor, **^{i}Pr-Py-BOX** as the chiral ligand, and 1,3-dichloro-5,5-dimethylhydantoin (DCDMH) as the chlorinating agent, one enantiomer of the racemic substrate **63** undergoes asymmetric chlorinative dearomatization in dichloromethane at −20 °C, converting the intrinsic $C(sp^2)$–$C(sp^2)$ axial chirality into chlorine-containing, conformationally stable $C(sp^2)$–$C(sp^3)$ axial chirality. A prominent advantage of this method is its excellent substrate compatibility, covering more than 30 derivatives of 1-aryl-2-naphthols **63**. In terms of functional groups, halogens, ethers, nitro groups, sulfonamides, alkenyl groups, alkynyl groups, *etc.*, are all well tolerated; even functional groups sensitive to metal catalysis show good stability. The ring skeletons are extended to

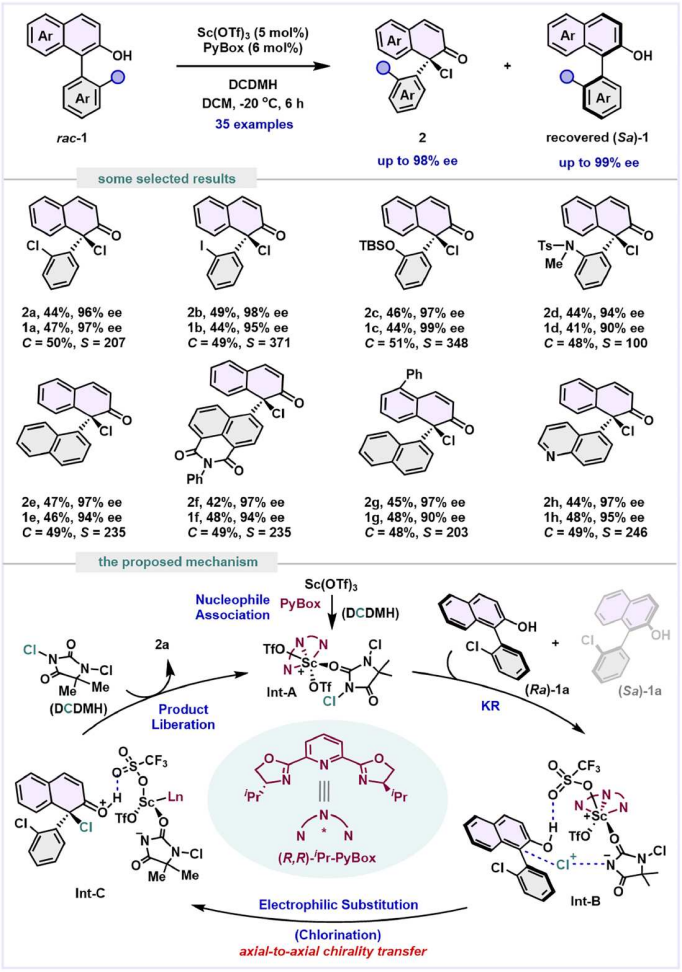

Figure 22 (Color online) Catalytic enantioselective chlorinative dearomatization of 1-aryl-2-naphthols.

fluorenyl, carbazole, benzofuran, phenanthrol, quinolinol, *etc*., with only 2′,6′-disubstituted substrates inactive due to excessive steric hindrance. The maximum resolution selectivity factor reaches 458, and the enantioselectivity of the dearomatized products **64** and recovered substrates (*Sa*)-**63** is up to 98% and 99% ee, respectively. In addition, the stereospecific dechlorinative rearomatization proceeds under blue-light irradiation, where dechlorination occurs to precisely transfer the stored chirality back to the original C(sp^2)–C(sp^2) axial chirality, achieving full resolution.

Mechanistic studies combined with DFT calculations and experimental verification reveal the origin of stereoselectivity. In the chlorination step, Sc(III) forms the active species Int-A with the **^{i}Pr-Py-BOX** ligand and DCDMH. The active species formed by Sc (III) and the ligand selectively recognizes one enantiomer (*Ra*)-**63a** through hydrogen bonding (OH···OTf) and steric repulsion effects, forming the axially chiral intermediate (*Ra*)-Int-B. Subsequently, intramolecular electrophilic substitution leads to the formation of the axially chiral intermediate (*Ra*)-Int-C. Finally, product dissociation and catalyst regeneration are achieved under the action of the chlorinating agent, completing the catalytic cycle.

4 Summary and outlook

The catalytic enantioselective synthesis via transient atropisomer axial chirality transfer strategy has not only emerged as a powerful tool for the precise construction of chiral spirocycles, fluorenols and/or atropisomers, but also represents a highly promising cutting-edge research direction in the field of modern asymmetric synthesis. This review systematically outlines the complete development trajectory of this strategy from its conceptual inception in 2015 to the present, focusing on the core reaction processes of metal-catalyzed chirality transfer from transient atropisomer axial chirality to central chirality or axial chirality. For the first time, we systematically classify these reactions into nine major categories based on the intrinsic chirality transfer mechanism: deprotonation, reductive elimination, alkene insertion, carbonyl insertion, imine insertion, nucleophilic attack, oxidation, isomerization, C–H insertion and electrophilic attack. Meanwhile, we further elaborate on the research advances in axial-to-axial chirality transfer achieved via two reaction pathways, namely reductive elimination and electrophilic attack, fully presenting the milestone achievements in this field and the expanding boundaries of its methodological development.

This strategy fundamentally breaks the inherent bottleneck of traditional chirality transfer strategies that rely heavily on pre-synthesized enantiopure substrates. Using readily available, low-cost racemic or prochiral precursors as starting materials, it generates configurationally tunable transient axially chiral intermediates *in situ* as chirality relay units through precise stereo-induction by chiral catalysts, ultimately enabling the high-fidelity transfer of chiral information from the catalyst to the target stereogenic site. Meanwhile, it combines excellent step economy, atom economy, and stereoselectivity, and is highly compatible with the requirements for efficient synthesis of complex functional molecules. Based on the full series of reaction systems summarized in this review, we summarize three core governing principles in this field: the generation and configurational stability of transient atropisomeric intermediates are the core prerequisite for efficient chirality transfer; the steric hindrance effect and noncovalent interactions of chiral ligands are the key determinant for stereoselectivity regulation; and solvent polarity, reaction temperature, and additives exert an indispensable regulatory effect on the regioselectivity of the reaction and the configurational stability of the intermediates.

Although a series of milestone breakthroughs have been achieved in this field, key scientific challenges remain to be addressed. In particular, due to the inherent properties of transient atropisomeric intermediates (short lifetime, low *in-situ* concentration, and easy racemization), there are significant technical barriers to their precise capture and direct characterization. As a result, their core role in stereochemical control and the underlying regulatory mechanism have not yet been systematically and comprehensively elucidated. In addition, current catalytic systems are still dominated by precious metals (Pd, Rh), the substrate scope of partial reactions is limited by substituent effects, and the practical application of this strategy in the total synthesis of complex molecules and industrial production remains largely unexplored.

Future research in this field should focus on three core directions: First, promoting the in-depth integration of advanced experimental characterization techniques and theoretical calculations to overcome the technical challenges in the precise capture of transient intermediates, and systematically elucidate the stereoregulatory mechanism throughout the entire chirality transfer process. Second, developing earth-abundant base-metal catalytic systems and novel chiral ligands, expanding transfer modes from axial chirality to novel stereogenic elements such as helical chirality and planar chirality, and achieving the precise and controllable construction of complex molecules bearing multiple stereocenters and diverse stereogenic elements. Third, focusing on the core applications of this strategy in the total synthesis of complex natural products, the preparation of key pharmaceutical intermediates,

and the synthesis of chiral ligands and functional materials, developing highly stable immobilized catalysts and continuous-flow synthetic processes, and driving the practical translation of this strategy from laboratory-scale methodological research to industrial applications.

Conflict of interest

The authors declare no conflict of interest.

Acknowledgement

This work was supported by the National Natural Science Foundation of China (22401293) and the National Key R&D Program of China (2021YFF0701600). We also dedicate this review to the 100th anniversary of the Department of Chemistry at Fudan University, celebrating its century-long outstanding contributions to the development of chemistry education and research.

References

1 LaPlante SR, Edwards PJ, Fader LD, Jakalian A, Hucke O. *ChemMedChem*, 2011, 6: 505–513
2 LaPlante SR, Fader LD, Fandrick KR, Fandrick DR, Hucke O, Kemper R, Miller SPF, Edwards PJ. *J Med Chem*, 2011, 54: 7005–7022
3 Oki M. *Top Stereochem*, 1983, 14: 1–81
4 Kozlowski MC, Miller SJ, Perreault S. *Acc Chem Res*, 2023, 56: 187–188
5 Christie GH, Kenner J. *J Chem Soc Trans*, 1922, 121: 614–620
6 Alonso JM, Quirós MT, Muñoz MP. *Org Chem Front*, 2016, 3: 1186–1204
7 Patil NT. *Chem Asian J*, 2012, 7: 2186–2194
8 Pizzolato SF, Štacko P, Kistemaker JCM, van Leeuwen T, Otten E, Feringa BL. *J Am Chem Soc*, 2018, 140: 17278–17289
9 Nguyen TT. *Org Biomol Chem*, 2019, 17: 6952–6963
10 Yang H, Chen J, Zhou L. *Chem Asian J*, 2020, 15: 2939–2951
11 Min XL, Zhang XL, Shen R, Zhang Q, He Y. *Org Chem Front*, 2022, 9: 2280–2292
12 Lemaitre C, Perulli S, Quinonero O, Bressy C, Rodriguez J, Constantieux T, García Mancheño O, Bugaut X. *Molecules*, 2023, 28: 3142
13 Chang H, Wang R, Wang Y. *Chem Asian J*, 2025, 20: e00105
14 Yang H, Feng H, Zhou L. *Eur J Org Chem*, 2024, 27: e202400671
15 Ito T, Tsutsumi M, Yamada K, Takikawa H, Yamaoka Y, Takasu K. *Angew Chem Int Ed*, 2019, 58: 11836–11840
16 Campolo D, Gastaldi S, Roussel C, Bertrand MP, Nechab M. *Chem Soc Rev*, 2013, 42: 8434–8466
17 Neff RK, Frantz DE. *Tetrahedron*, 2015, 71: 7–18
18 Murai T. *Chem Lett*, 2023, 52: 703–714
19 Myllek S, Lencer P, Klischan MKT, Henssen B, Neudecker P, Breugst M, Pietruszka J. *Org Biomol Chem*, 2025, 23: 4888–4892
20 Fan P, Li L, Qian D. *Org Biomol Chem*, 2024, 22: 3186–3197
21 Walsh PJ, Kozlowski MC. *Fundamentals of Asymmetric Catalysis*. Sausalito: University Science Books, 2009
22 Ojima I. *Catalytic Asymmetric Synthesis*. Hoboken: John Wiley & Sons, 2010
23 Yang L, Zheng H, Luo L, Nan J, Liu J, Wang Y, Luan X. *J Am Chem Soc*, 2015, 137: 4876–4879
24 Zheng J, Wang SB, Zheng C, You SL. *J Am Chem Soc*, 2015, 137: 4880–4883
25 Bringmann G, Gulder T, Gulder TAM, Breuning M. *Chem Rev*, 2011, 111: 563–639
26 Xiang SH, Ding WY, Wang YB, Tan B. *Nat Catal*, 2024, 7: 483–498
27 Zhang H, Li T, Liu S, Shi F. *Angew Chem Int Ed*, 2024, 63: e202311053
28 Schmidt TA, Hutskalova V, Sparr C. *Nat Rev Chem*, 2024, 8: 497–517
29 Rodríguez-Salamanca P, Fernández R, Hornillos V, Lassaletta JM. *Chem Eur J*, 2022, 28: e202104442
30 Roos CB, Chiang CH, Murray LAM, Yang D, Schulert L, Narayan ARH. *Chem Rev*, 2023, 123: 10641–10727
31 Bhat V, Welin ER, Guo X, Stoltz BM. *Chem Rev*, 2017, 117: 4528–4561
32 Zhang Y, Cai H, Gan X, Jin Z. *Sci China Chem*, 2024, 67: 482–511
33 Xu PW, Yu JS, Chen C, Cao ZY, Zhou F, Zhou J. *ACS Catal*, 2019, 9: 1820–1882
34 Zhao Q, Peng C, Wang YT, Zhan G, Han B. *Org Chem Front*, 2021, 8: 2772–2785
35 Ding A, Meazza M, Guo H, Yang JW, Rios R. *Chem Soc Rev*, 2018, 47: 5946–5996
36 Luo X, Zhong K, Lan Y. *ChemCatChem*, 2020, 12: 3863–3869
37 Zheng C, You SL. *ACS Cent Sci*, 2021, 7: 432–444
38 Zheng C, You SL. *Chem*, 2016, 1: 830–857
39 You Y, Yu SL, Li Q, Zhang YP, Wang ZH, Zhao JQ, Yang L, Yuan WC. *ACS Catal*, 2025, 15: 9503–9543
40 Zheng C, Zheng J, You SL. *ACS Catal*, 2016, 6: 262–271
41 Reddy Chidipudi S, Burns DJ, Khan I, Lam HW. *Angew Chem Int Ed*, 2015, 54: 13975–13979
42 Fan L, Liu J, Bai L, Wang Y, Luan X. *Angew Chem Int Ed*, 2017, 56: 14257–14261
43 Bai L, Liu J, Hu W, Li K, Wang Y, Luan X. *Angew Chem Int Ed*, 2018, 57: 5151–5155
44 Hiesinger K, Dar'in D, Proschak E, Krasavin M. *J Med Chem*, 2021, 64: 150–183
45 Tian Q, Ge J, Liu Y, Wu X, Li Z, Cheng G. *Angew Chem Int Ed*, 2024, 63: e202409366
46 Cheng H, Chen S, Chen R, Zhou Q. *Angew Chem Int Ed*, 2019, 58: 5832–5844
47 Wu C, Zhu J, Li W. *Chem Eur J*, 2026, 32: e03561
48 Gangwar H, Azeem Z, Kumar Mandal P. *Adv Synth Catal*, 2025, 367: e202401570
49 Wang J, Dong G. *Chem Rev*, 2019, 119: 7478–7528
50 Della Ca' N, Fontana M, Motti E, Catellani M. *Acc Chem Res*, 2016, 49: 1389–1400
51 Chu H, Cheng J, Yang J, Guo Y, Zhang J. *Angew Chem Int Ed*, 2020, 59: 21991–21996
52 Li W, Zhang J. *Acc Chem Res*, 2024, 57: 489–513
53 Yu S. *Chem Asian J*, 2025, 20: e202500023
54 Zhang LZ, Zhang PC, Wang Q, Zhou M, Zhang J. *Nat Commun*, 2025, 16: 930
55 Xu B, Ji D, Zhang Z, Zhang J. *Adv Sci*, 2024, 11: 2406443
56 Feng J, Shi J, Wei L, Liu M, Li Z, Xiao Y, Zhang J. *Angew Chem Int Ed*, 2023, 62: e202215407
57 Zhang W, Zhang PC, Li YL, Wu HH, Zhang J. *J Am Chem Soc*, 2022, 144: 19627–19634
58 Xu B, Ji D, Wu L, Zhou L, Liu Y, Zhang ZM, Zhang J. *Chem*, 2022, 8: 836–849
59 Li YL, Zhang PC, Wu HH, Zhang J. *J Am Chem Soc*, 2021, 143: 13010–13015
60 Zhang P, Han J, Zhang J. *Angew Chem Int Ed*, 2019, 58: 11444–11448
61 Zhang JT, Wang HY, Zhu W, Cai TT, Guo YL. *Anal Chem*, 2014, 86: 8937–8942
62 Gao D, Jiao L. *Angew Chem Int Ed*, 2022, 61: e202116024
63 Rössler SL, Petrone DA, Carreira EM. *Acc Chem Res*, 2019, 52: 2657–2672
64 Han L, Cui Y, Yang Q, Fang L, Xu L. *Angew Chem Int Ed*, 2022, 61: e202211922
65 Li YH, Ouyang Y, Yan JL, Chekshin N, Yu JQ. *Acc Chem Res*, 2025, 58: 2910–2926
66 Phukon J, Jyoti Borah A, Gogoi S. *Asian J Org Chem*, 2022, 11: e202200581
67 Yang K, Song M, Liu H, Ge H. *Chem Sci*, 2020, 11: 12616–12632
68 Takano H, Kanyiva KS, Shibata T. *Org Lett*, 2016, 18: 1860–1863
69 Takano H, Ito T, Kanyiva KS, Shibata T. *Eur J Org Chem*, 2019, 2019: 2871–2883
70 Takano H, Sugimura N, Kanyiva KS, Shibata T. *ACS Omega*, 2017, 2: 5228–5234
71 Liu ZS, Hua Y, Gao Q, Ma Y, Tang H, Shang Y, Cheng HG, Zhou Q. *Nat Catal*, 2020, 3: 727–733
72 Li C, Liu L, Fu X, Huang J. *Synthesis*, 2018, 50: 2799–2823
73 Cao K, Yuan B, Liu X, Wu MF, Yao Z. *Prog Chem*, 2017, 29: 605–616
74 Shi H, Herron AN, Shao Y, Shao Q, Yu JQ. *Nature*, 2018, 558: 581–585
75 Ding B, Xue Q, Wei H, Chen J, Liu ZS, Cheng HG, Cong H, Tang J, Zhou Q. *Chem Sci*, 2024, 15: 7975–7981
76 Casnati A, Fontana M, Motti E, Della Ca' N. *Org Biomol Chem*, 2019, 17: 6165–6173
77 Muzart J. *Tetrahedron*, 2003, 59: 5789–5816
78 Ou T, Xiang L, Zhou Y, Jiang F, Wang X, Guo W. *Eur J Org Chem*, 2024, 27: e202400795
79 Li W, Zheng Y, Gu Y, Cheng S, Xie J, Lu Y, Chen S, Song Q. *Angew Chem Int Ed*, 2025, 64: e202506873
80 Yang K, Song Q. *Acc Chem Res*, 2021, 54: 2298–2312
81 Kuang Z, Yang K, Zhou Y, Song Q. *Chem Commun*, 2020, 56: 6469–6479
82 Li W, Chen S, Xie J, Fan Z, Yang K, Song Q. *Nat Synth*, 2023, 2: 140–151
83 Yang P, Wang Q, Cui BH, Zhang XD, Liu H, Zhang YY, Liu JL, Huang WY, Liang RX, Jia YX. *J Am Chem Soc*, 2022, 144: 1087–1093
84 Ni Q, Chen Y, Ma Y. *Synthesis*, 2025, 57: 2289–2306
85 Zhang X, Li D, Tian Y, Zhong Y, Liu W, Wang Y, Huang W, Zhan G, Li J. *Green Synth Catal*, 2025, doi: 10.1016/j.gresc.2025.05.012
86 Lu C, Hao B, Han Y, Liang Y. *Asian J Org Chem*, 2022, 11: e202200312
87 Lou SJ, Luo G, Yamaguchi S, An K, Nishiura M, Hou Z. *J Am Chem Soc*, 2021, 143: 20462–20471
88 Mishra A, Cong X, Nishiura M, Hou Z. *J Am Chem Soc*, 2023, 145: 17468–17477
89 Gandeepan P, Cheng CH. *Acc Chem Res*, 2015, 48: 1194–1206
90 Su L, Gao S, Liu J. *Nat Commun*, 2025, 16: 9559
91 Qian C, Liu M, Sun J, Li P. *Org Chem Front*, 2022, 9: 1234–1240
92 Unhale RA, Sadhu MM, Singh VK. *Org Lett*, 2022, 24: 3319–3324
93 Shu X, Zhang T, Zhang Y, Tong K, Wang S, Wang Y. *Org Chem Front*, 2025, 12: 3643–3648
94 Liu F, Guo Y, Lu W, Zhao X, Yin Y, Jiang Z. *Chem Sci*, 2025, 16: 10555–10562
95 Luo L, Zheng H, Liu J, Wang H, Wang Y, Luan X. *Org Lett*, 2016, 18: 2082–2085
96 Zhao G, Li W, Zhang J. *Chem Eur J*, 2024, 30: e202400076
97 Li H, Gontla R, Flegel J, Merten C, Ziegler S, Antonchick AP, Waldmann H. *Angew Chem Int Ed*, 2019, 58: 307–311
98 Zheng J, Wang S, Zheng C, You S. *Angew Chem Int Ed*, 2017, 56: 4540–4544
99 Kong L, Han X, Liu S, Zou Y, Lan Y, Li X. *Angew Chem Int Ed*, 2020, 59: 7188–7192
100 Liu J, Liang R, Yan Q, Zheng L, Liu ZQ, Pu S. *Org Chem Front*, 2025, 12: 3065–3106
101 Pan C, Yin SY, Gu Q, You SL. *Org Biomol Chem*, 2021, 19: 7264–7275
102 Kong KX, Zhou T, Yuan WK, Hui XS, Li Y, Shi BF. *ACS Catal*, 2025, 15: 4280–4286
103 Sumit, Chandra D, Sharma U. *Chem Commun*, 2023, 59: 9288–9300
104 Shao Y, Cheng D. *ChemCatChem*, 2021, 13: 1271–1289
105 Zhan BB, Jin L, Shi BF. *Trends Chem*, 2022, 4: 220–235
106 Vyhivskyi O, Kudashev A, Miyakoshi T, Baudoin O. *Chem Eur J*, 2021, 27: 1231–1257
107 Liu CX, Zhang WW, Yin SY, Gu Q, You SL. *J Am Chem Soc*, 2021, 143: 14025–

14040
108 Liang Y, Zhou H, Yu ZX. *J Am Chem Soc*, 2009, 131: 17783–17785
109 Dong K, Fan X, Pei C, Zheng Y, Chang S, Cai J, Qiu L, Yu ZX, Xu X. *Nat Commun*, 2020, 11: 2363
110 He Y, Huang Z, Wu K, Ma J, Zhou YG, Yu Z. *Chem Soc Rev*, 2022, 51: 2759–2852
111 Bergstrom BD, Nickerson LA, Shaw JT, Souza LW. *Angew Chem Int Ed*, 2021, 60: 6864–6878
112 Wu R, Xu Z, Zhu D, Zhu S. *Acc Chem Res*, 2025, 58: 799–811
113 Li T, Leng D, Niu JL, Hu XH, Loh TP. *Top Curr Chem (Z)*, 2026, 384: 6
114 Kitagawa O. *J Org Chem*, 2024, 89: 11089–11099
115 Mei GJ, Koay WL, Guan CY, Lu Y. *Chem*, 2022, 8: 1855–1893
116 Liu ZS, Xie PP, Hua Y, Wu C, Ma Y, Chen J, Cheng HG, Hong X, Zhou Q. *Chem*, 2021, 7: 1917–1932
117 Wu C, Liu Z, Shang Y, Liu C, Deng S, Cheng H, Cong H, Jiao Y, Zhou Q. *Chin J Chem*, 2024, 42: 699–704
118 Zhao D, Sun J, Chen N, Ge Y, Liu J, Bai L, Luan X. *J Am Chem Soc*, 2025, 147: 23202–23212
119 Yin Q, Wang SG, Liang XW, Gao DW, Zheng J, You SL. *Chem Sci*, 2015, 6: 4179–4183
120 Zhou Y, Ping Y, Xu Z, Che C. *Asian J Org Chem*, 2021, 10: 674–678
121 Zhang N, Chen Y, Qian G, Ge Y, Zhao D, Liu L, Bai L, Hong X, Liu J, Luan X. *J Am Chem Soc*, 2025, 147: 46384–46395